Site Visit and Drone Based Reconnaissance Study of the Severely Affected Infrastructure by February 7th, 2021, Chamoli Rock-Ice Avalanche Disaster, Uttarakhand, India

Barrage of Tapovan Vishnugad hydroelectric project

GEER – 074
doi:10.18118/G6V95B

Reconnaissance Team and Authors:

Prashanth Vangla, Assistant Professor, IIT Delhi, India
Dipali Jindal, Ph.D. Student, IIT Delhi, India
Avinash Sajwan, Ph.D. Student, IIT Delhi, India
Rituraj Devrani, Ph.D. Candidate, IIT Delhi, India

Reconnaissance Coordinators and Authors (in alphabetical order):

J. David Frost, Elizabeth and Bill Higginbotham Professor, Georgia Institute of Technology, USA
G. V. Ramana, Professor, IIT Delhi, India

Other Contributors (in alphabetical order):

Alejandro Martinez, University of California Davis, USA
Biruk Gissila, Ph.D Candidate, IIT Delhi, India
C. T. Dhanya, IIT Delhi, India
G. Madhavi Latha, IISc, India
G.L.Sivakumar Babu, IISc, India
G. S. P, Madabhushi, University of Cambridge, UK
E. Nichols, GEER Recorder, Georgia Institute of Technology
K. S. Rao, IIT Delhi, India
R. Ayothiraman, Professor, IIT Delhi, India
Sri Harsha Kota, IIT Delhi, India

Acknowledgments

This report is an outcome of a collaborative project supported by the Scheme for Promotion of Academic and Research Collaboration (SPARC) Project #P83, MoE, India at IIT Delhi. The sponsored collaborative project titled "*Advanced Technologies for Post-Disasters Reconnaissance, Forensic and Environmental Impact Studies - Geotechnical*" among IIT Delhi, IISc, Georgia Institute of Technology, University of California, Davis, and the University of Cambridge, mobilized a team from IIT Delhi to conduct a reconnaissance study to gather the perishable data of the February 07^{th,} 2021 Chamoli disaster.

Any opinions, findings, conclusions, or recommendations expressed in this report are those of the authors and do not necessarily reflect the views of the MoE. The reconnaissance team and coordinators would like to acknowledge and appreciate several officials, news reporters, locals of the Tapovan and Rishiganga areas who supported the reconnaissance team during the field trip. Our special thanks to Mr. Kundan Prasad, CO, ITBP., Mr. Benudhar Nayak, Commandant, ITBP, Mr. Sher Singh Butola, Assistant Commandant, ITBP, Mr. Ravi Kumar Yadav, GREF, Dr. Sunita Kumari, Associate Professor, NIT Patna, and other several officials of ITBP, for facilitating local logistics and permissions to access the affected areas for collecting all the crucial information for the recce. We especially appreciate Mr. Sher Singh Butola for his constant support and valuable aftermath insights into the study area he gathered through the aerial survey conducted with ITBP support. We also thank several locals who helped us during the recce study, special mentions to Mr. Sikim (brother of the NTPC staff, who was missing after the floods), who witnessed the event, explained the event's details, and its effects on the Rishiganga project. He also provided critical pre and post-event videos/photographs that are used in the report with his permission.

Contents

List of Figures

Statement of General Liability Limitation – Disclaimer

This reconnaissance mission team was comprised of individual volunteers. The findings and observations presented in this report are based on the conditions of the observed features at the time of the inspection and their experience with other similar structures. This report is not an assessment of the situation or safety of the structures observed. No warranty or guarantee regarding the performance or safety of the observed structures is included or intended. Any use of or reliance on this report is at the sole risk of the party using or relying on the report.

NSF Acknowledgement

The work of the GEER Association is based in part on work supported by the National Science Foundation through the Engineering for Civil Infrastructure Program under Grant No. CMMI1826118. Any opinions, findings, and conclusions or recommendations expressed in this material are those of the authors and do not necessarily reflect the views of the NSF.

Summary

This report documents the field observations made by the reconnaissance team during the site visit undertaken from February 9th through 11th, 2021, in the flash flood location in Chamoli District, Uttarakhand, India. The extreme event of the flash flood unfolded on 7th Feb 2021 and inundated the banks of the Rishiganga and Dhauliganga rivers with debris flow. The extreme event caused massive destruction to hydropower projects (Rishiganga HEP and Tapovan Vishnugad HEP), bridges, roads, houses, and out of a total of 204 missing persons, 78 people were reported dead as per the published document by the Disaster Management Division, Ministry of Home Affairs (https://ndmindia.mha.gov.in/NDMINDIA-CMS/viewsituationDisasterReportPdfDocument-103). Initially, it is speculated that a glacial lake outburst flood (GLOF) might have been the cause of the flash floods.However, subsequent analysis of satellite images revealed that a rock-ice avalanche caused debris flow and flash flood (Martha et al., 2021). This report doesn't present and discuss the causative factors of the disaster but focuses on collecting perishable data and damage assessment based on a drone-based reconnaissance study (Zwęgliński 2020). The planning and implementation of the reconnaissance study were by the IIT Delhi Team. The site visit is undertaken from February 9th through February 11th, 2021, two days after the event, as summarized in subsequent chapters.

Field reconnaissance involves capturing geo-referenced images of the affected areas through drones and digital cameras that provide direct information about the conditions on the ground to assess the consequences/damage resulting from the disaster. Digital Elevation Models (DEMs) of the affected areas, including upstream and downstream of Rishiganga HEP (R-HEP) and Tapovan Vishnugad HEP (TV-HEP), generated from the drone survey are used to describe the severity of damage to the hydropower infrastructure, flood height range and topographical variation due to floods. Further, the cross-sectional variation of the river valley of both the locations (R-HEP and

TV-HEP) is quantitatively analyzed using DEMs. The report also presents the geometrical features of the damaged structures and rock fragments/boulders (Collins 2014) that were rolled downstream by the flash floods. Additionally, the classification of soil samples collected with a hand auger from different locations at the Rishiganga site is presented. The report also highlights the importance and usefulness of pre and post-event images/videos obtained from the locals to locate and map the lost and damaged structures and get a qualitative gauge of the damage incurred. Some efforts are made to quantify the erosion, deposition, and topographical changes based on the observations made during the field reconnaissance and drone survey.

Chapter 1: Introduction

1.1 February 7th, 2021 Cascading Chamoli disaster

Chamoli lies in the north-eastern part of Uttarakhand state, India. A significant part of the district is always covered with snow. The topography of the Chamoli district has high hills and mountains with very narrow valleys, deep gorges having very high gradients. Several important rivers Alaknanda, and tributaries (Rishiganga and Dhauliganga) flow through this region. These rivers generally flow with high velocity in steep and narrow channels, often resulting in excessive erosion and collapse of the banks. Due to the cool and moist climate, the soils have developed from rocks like granite, schist, gneiss, phyllites, shales, and slate. Structural imbalances generally accompany the occurrence of groundwater in hilly areas. The state is prone to landslides, earthquakes, and floods due to these geological and physiographic features (Martha and Vinod Kumar 2013).

Around 10:22 am [IST], a catastrophic ice-rock avalanche that transformed into a mud and debris flood wave with extreme speed descended the Ronti Gad, Rishiganga, Tapovan, and Dhauliganga valleys in Chamoli district, Uttarakhand, India. It caused massive destruction of hydropower structures, roads, and bridges and killed several people along its path. Rishiganga and Tapovan Vishnugad hydropower projects were damaged severely. The disaster is the first of its kind in India. It can be classified as an extreme event for two reasons: 1) it is an enormous and devastating debris flood wave causing massive devastation, and 2) it opened up a new dimension for learning and provided an opportunity to review and redesign current policies for planning hydropower infrastructure in high hills and mountainous areas.

The satellite images (KOMPSAT 3A, SENTINEL 2A, and PLEIADES) that were released immediately after the event revealed that the source of the flash flood was found at Ronti Peak (Glacier Valley) at an altitude of about 5500 m Mean Sea Level (MSL). Figures 1.1a and 1.1b

present the satellite images of suspected rock-ice slide avalanche location (captured on 16th Sep 2020) and crack formation just before the event, i.e., 5th Feb 2021, respectively. The image presented in Figure 1.1(c), captured on 9th Feb 2021, clearly indicates that a massive and suspended site was dislodged, forming a vast cavity with approximate dimensions of 0.61 km wide and 1.32 km high. Figure 1.1(d) presents a 3D interpretation of the slide and its location. Figure 1.2 gives the overviews of the rock-ice avalanche travel path (bold blue line) from the event source to the point where the floodwater and debris were detained.

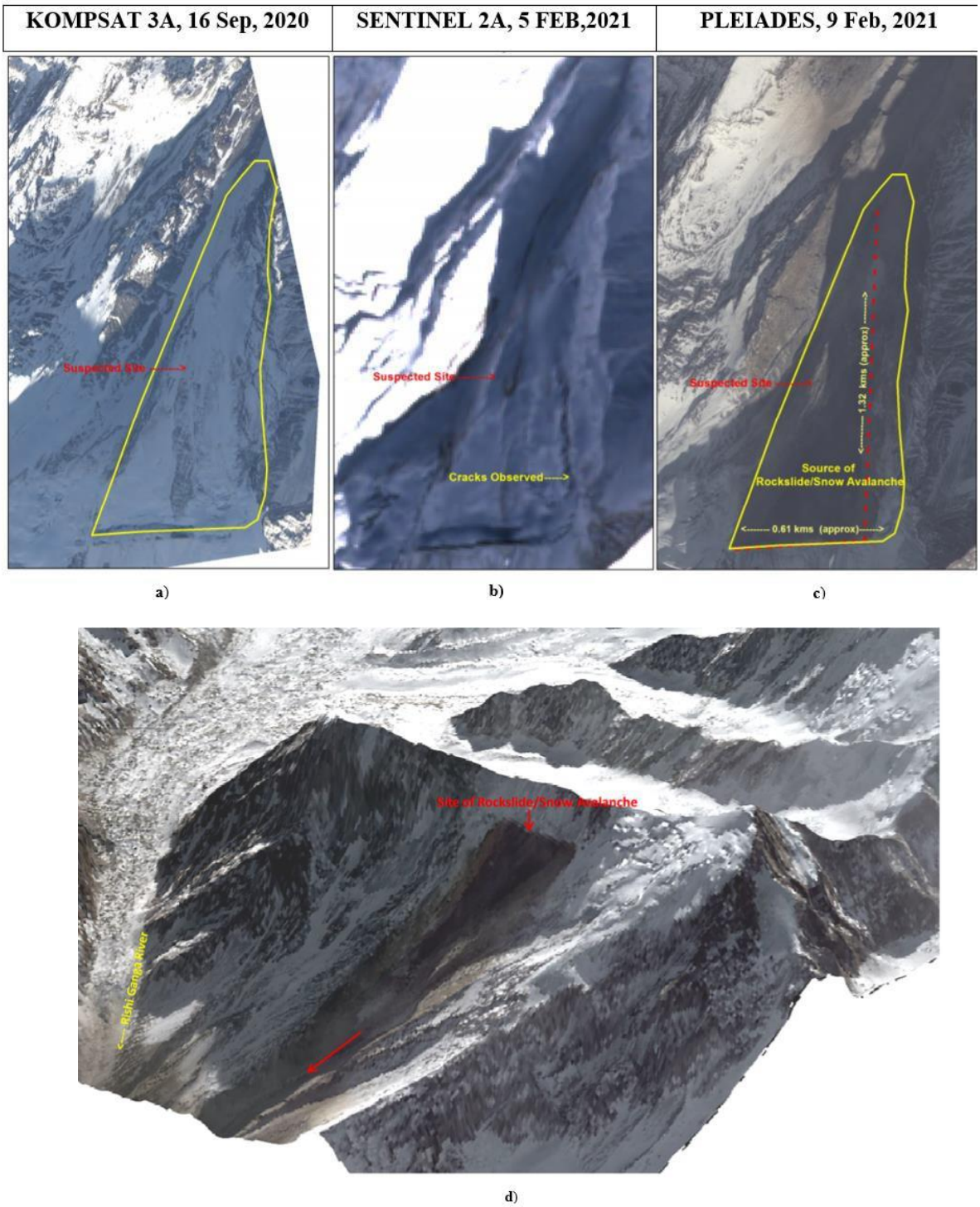

Figure 1.1 a) Suspected Site of Rockslide/Snow Avalanche (16 September 2020, source: KOMPSAT 3A) (b) Observed cracks (05 February 2021, source: SENTINEL 2A) (c) Crack width (source: PLEIADES) (d) 3D Rendition of the Suspected Area of Rockslide/Snow Avalanche (09-Feb2021, source: ISRO-CARTOSAT-3 satellite)

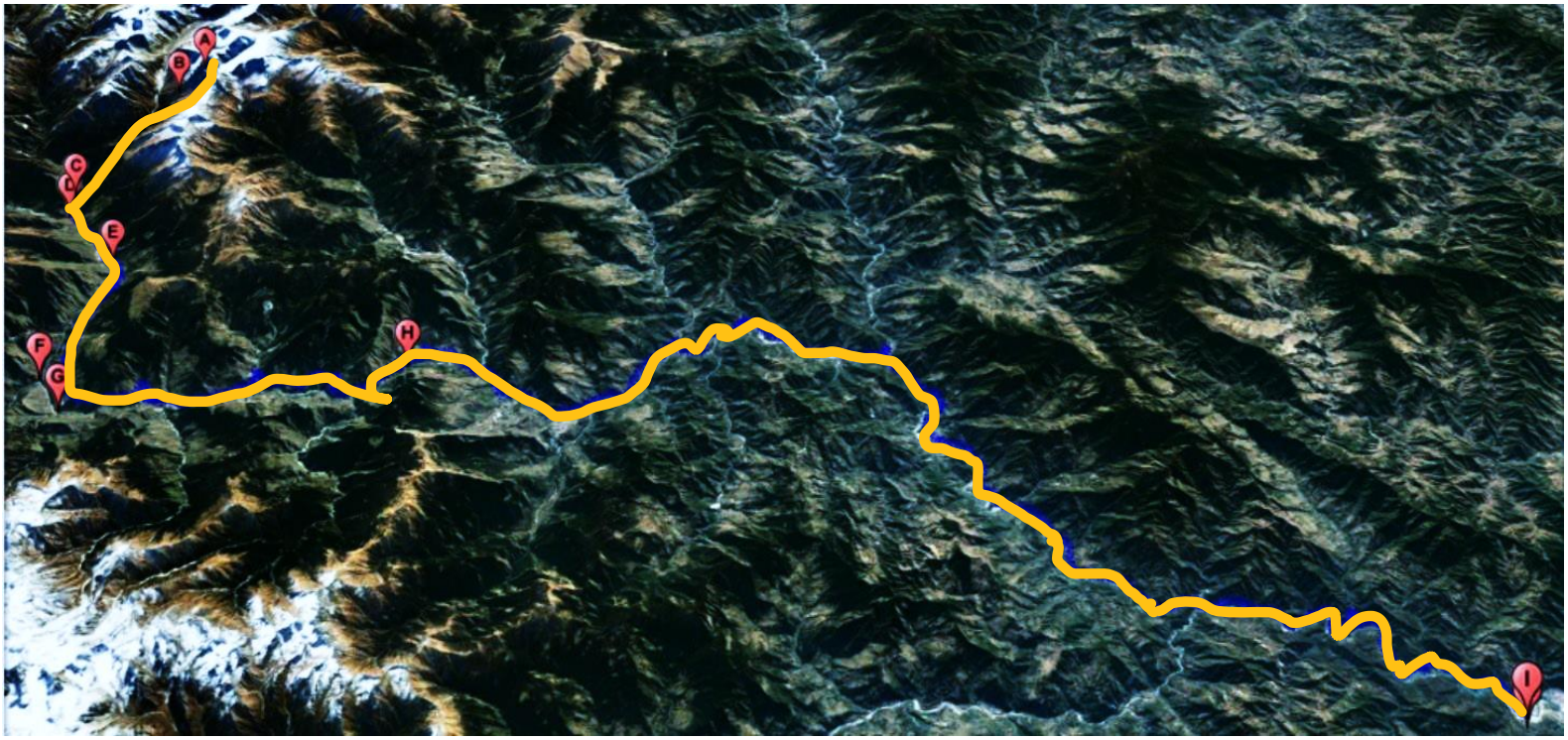

Figure 1.2 Overview of the rock-ice avalanche travel path (bold blue line) from the event source to the point where the floodwater and debris were detained.

A - Source of rock-ice avalanche (30°22'35.05"N, 79°42'59.15"E)
B - Ronti Gad (30°23'39.27"N, 79°43'18.71"E)
C - Rishiganga HEP (30°28'42.04"N, 79°41'59.65"E)
D - Confluence: Rishiganga and Dhauliganga (30°29'17.54"N, 79°41'24.47"E)
E - Tapovan HEP (30°29'32.85"N, 79°37'52.51"E)
F - Confluence: Dhauliganga and Alaknanda (30°33'44.68"N, 79°34'33.99"E)
G - Vishnuprayag HEP (30°34'1.09"N, 79°32'48.56"E)
H - Vishnuprayag Pipalkoti HEP (30°25'58.80"N, 79°25'26.40"E)
I – Srinagar Dam/ Alaknanda HEP (30°14'31.28"N, 78°49'20.41"E)

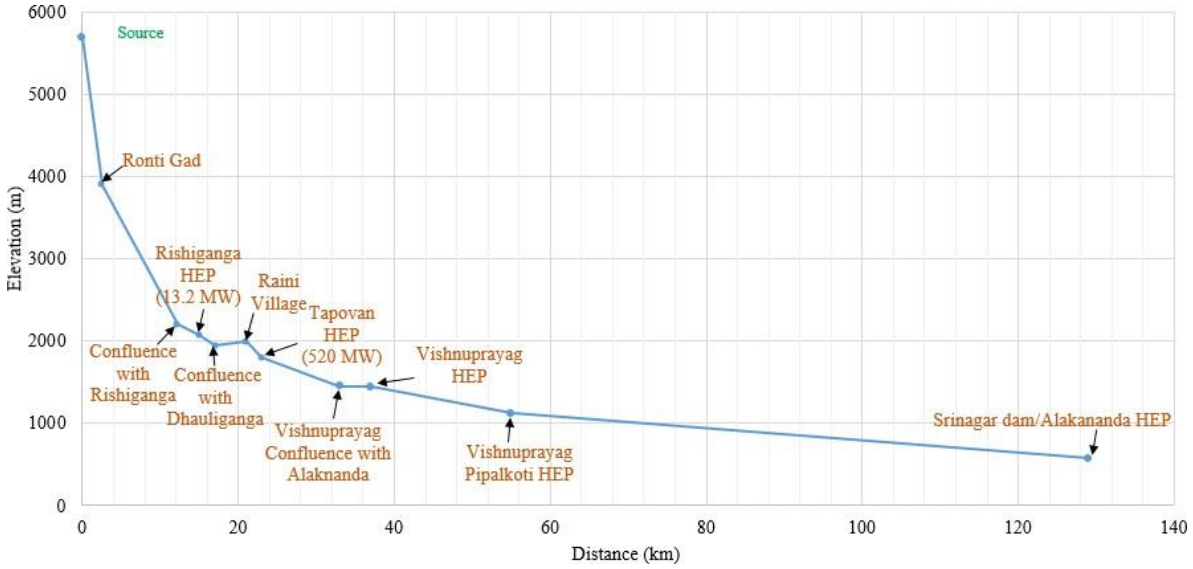

Figure 1.3 Distance and elevation difference of different affected areas from the source of rock-ice avalanche

Figure 1.3 depicts the distance and elevation difference of different hydropower projects and rivers from the source of the rock-ice avalanche. One can imagine the impact and the intensity of the damage incurred by hydroelectric projects and associated structures due tothe flash flood. The first interaction of dislodged mass with the ground surface was with a small stream through which the glacier drains, i.e., Ronti Gad, at a distance of approximately 1.6 km and about an elevation of 1800 m below the source. Then it traveled along the valley of Ronti Gad and mixed with Rishiganga River, a source for the 13.2 MW Rishiganga hydroelectric project (HEP) near Raini Village at an approximate distance of 15 km with an elevation difference of 3631m from the impact (source) site. It is the first HEP to face the brunt of the intense rock-ice avalanche. Most its structures/components were swept away and buried. Debris from R-HEP damaged other units downstream and several megastructures, including one of the essential RCC bridges at Rishiganga

(1985 above mean sea level) in the neighborhood of Dhauliganga (at a distance and elevation of about 17 km and 3755 m from the source site). TV-HEP (520 MW, under construction) at Dhauliganga, approx. 8 km downstream of R-HEP, and 23 km from the impact site, tap the river water of Rishiganga and Dhauliganga. This second hydroelectric plant was impacted by flash floods which contained large amounts of mud, debris, and large chunks of concrete/rock. The Dhauliganga river, after the confluence with Rishiganga river, joins Alaknanda at Vishnuprayag (confluence: 4247m elevation, and 33 km distance from the slide location), is the source river for two power projects along the way, namely, Vishnuprayag Hydro Electric Project (400 MW, operational) and Vishnugad Pipalkoti Hydro Electric Project (444 MW, under construction). These two HEPs have received minor to no damage. The Srinagar dam of Alaknanda HEP, located at about 129 km and 5126 m elevation below the source, received and detained the debris and floodwater produced by the avalanche (Figure 1.4.)

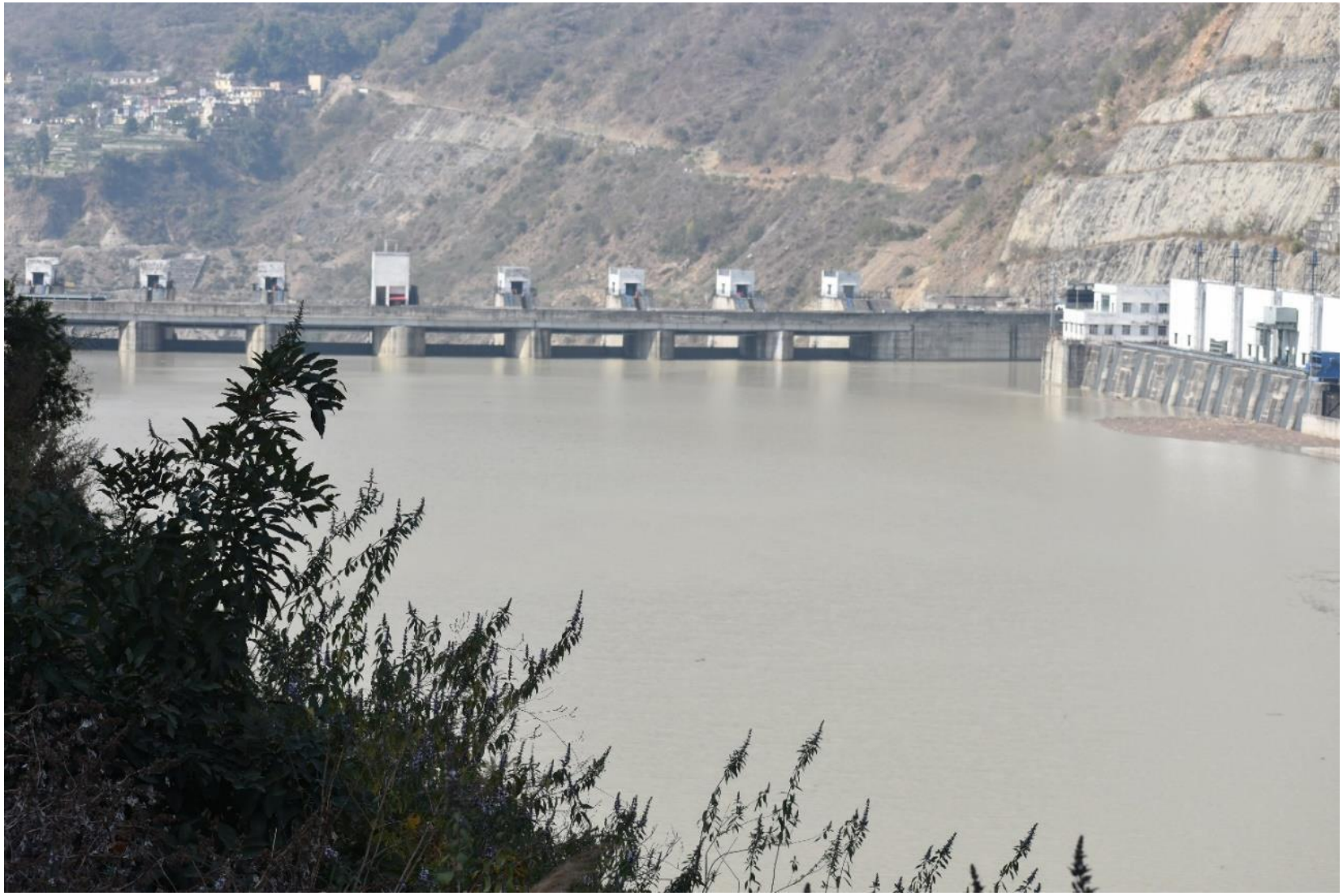

Figure 1.4 Srinagar Dam with turbid water (Dated 11/02/2021) (30°14'31.28"N, 78°49'20.41"E)

Chapter 2: Reconnaissance survey

2.1 Planning and Implementation

The team planned their initial route map to visit the locations affected by the Chamoli disaster, based on preliminary information gathered from social media and news reports. The Google Earth Pro and Maps of India were utilized to locate the affected areas, including details about hydropower projects, bridges, houses, roads, and flash flood travel paths. It was also learned that some of the severely affected regions were partly inaccessible. The objective of the reconnaissance study was to get a first-hand view and collect the perishable data of the areas that are severely affected by disaster (Wartman et al., 2020), which could be used to understand the response of and damage to the infrastructure in these areas. To this end, the team decided to primarily conduct drone-basedreconnaissance and collect the soil samples at possible locations.

The team traveled to Chamoli district on February 9^{th,} 2021, and reached in the evening on February 10th and stayed at the nearest location of the affected areas, i.e., Joshimath. The areasto be studied were decided, namely, Rishiganga HEP and Tapovan HEP, after learning from thelocals and government officials that these places were severely affected and further confirmed through the field visit by the team. Early at 6:00 am on February 11th, the team first visited the Rishiganga HEP area, which was severely affected due to its proximity to the avalanche source. A drone imagery survey was conducted, covering approximately 41.9 hectares along the Rishigangariver stretch. The starting location of the survey is at 30°28'18.40"N, 79°42'26.66"E and the ending location at 30°29'19.42"N, 79°41'24.60"E upstream and downstream of Rishiganga river, respectively. The team also collected soil samples from this location for soil characterization. On the same day, in the afternoon, the team traveled 8 km downstream of R-HEP to the second hydropower project along the travel path of flash floods, i.e., Tapovan HEP, at Dhauliganga. The

aerial survey carried out in this area spanned between 30°29'43.16"N, 79°37'25.53"E and 30°29'31.65"N, 79°37'54.99"E, covering an area of about 11.8 hectares. In addition to drone surveys and sample collections, the team also collected valuable information from the locals that witnessed and captured the event using smartphones and cameras.

2.2 Equipment and tools

In this reconnaissance study, the team used state-of-the-art as well as conventional equipment and tools to accomplish the objectives systematically. The details of the equipment used in the study are given below.

Equipment and tools:

- Drone
  - TALV2400- RPASF (Flight altitudes above ground level (AGL) 70 m)
- Differential Global Positioning System (DGPS)
  - EMLID RS2 DGPS was used for establishing Ground Control Points (GCP)
  - Ground sample distance (GSD) considered was 3 cm.
- DSLR Camera
- Rugged Handheld Garmin GPS (eTrex® 10)
- Extendable Auger Soil Samplers, pick-ax, and construction spade.

Chapter 3: Impacts on the infrastructure in the study areas

The impacts on the infrastructure of two locations, namely, Rishiganga HEP/Raini village and Tapovan, that were severely affected by the rock-ice avalanche, are discussed in the following sections.

3.1 Study Area – I: Rishiganga HEP and Raini Bridge

The first reconnoitered area consisted of several vital infrastructures, including a barrage, impoundment, and components of the hydropower plant, roads, and a reinforced concretebridge, as shown in Figure 3.1a. Figure 3.1b presents the post-event orthophoto generated from the drone survey of the same area. The hydroelectric project commissioned in September 2012 was a Run-of-River (RoR) with a capacity of 13.2 MW on the Rishiganga River, expected to generate approximately 59,031 MWh (net) electricity per annum, and was completely damaged. The RCC Bridge is a crucial and necessary structure connecting the two parts of the Raini village and links 13 villages close to the border with China that got completely washed away. Along with these structures, several other associated and supporting buildings of HEP and connecting roads also suffered severe damage, as shown in Figure 3.1b, due to the flash floods. Figures 3.2-3.4 give the close-up view images of the REP and Raini bridge components collected from the locals. Figure 3.2 presents the impoundment connected to the diversion tunnel before and after fillingthe water. Figure 3.3 shows staff quarters, office buildings, and some utility structures of the powerplant before the event. The powerhouse, penstock, and three-story building are on the Rishigangariver left bank. Figure 3.4 presents an inside view of the power plant. These structures were destroyed and thus missing after the disaster (Figure 3.1b).

(a)

(b)

Figure 3.1 Status of Infrastructure in the Rishiganga HEP location before and after the event. The locations of the structures are marked by solid yellow line shapes a) Google Earth imagery, November 2018. b) ortho-imagery from drone survey, February 11th, 2021

(a)

(b)

Figure 3.1 Impoundment connected to the diversion tunnel a) during the construction b) after filling the water (Photo courtesy: Sikim, native) 30°28'45.39"N 79°41'53.46" E

(a)

(b)

Figure 3.2 Powerhouse, three-story building on Rishiganga river left bank and RCC bridge connecting Niti Valley a) from right bank road connecting to RCC bridge b) from penstock location (Photo courtesy: Sikim, native) @30°29'5.11"N 79°41'40.46"E

Figure 3.3 Inside view of the powerhouse(Photo courtesy: Sikim, native) @30°29'5.11"N 79°41'40.46" E

3.1.1 Photogrammetric evidence of Rishiganga-HEP and Raini village

A 3D aerial view downstream and upstream of HEP is presented in Figure 3.5, developed using the DEM draped by the mosaic images captured by the drone. Figure 3.6a illustrates the 3D perspective view and locations of prominent features before the event that existed in the study area. The features/structures at this location, barrage, and impoundment, temporary buildings, powerhouse, and bridge, are marked as A, B, C, and D, respectively, as shown in Figure 3.6a. Figure 3.6b presents the A, B, C, and D locations pre and post-event appearance. The comparison of pre (obtained from the Google imagery data) and post-event have shown in Figure 3.6b illustrates the extent of damage to the infrastructure.

Figure 3.4 Three-dimensional aerial view of the study area-I generated from its DEM draped by the mosaic image. (Dated: February 11th, 2021)

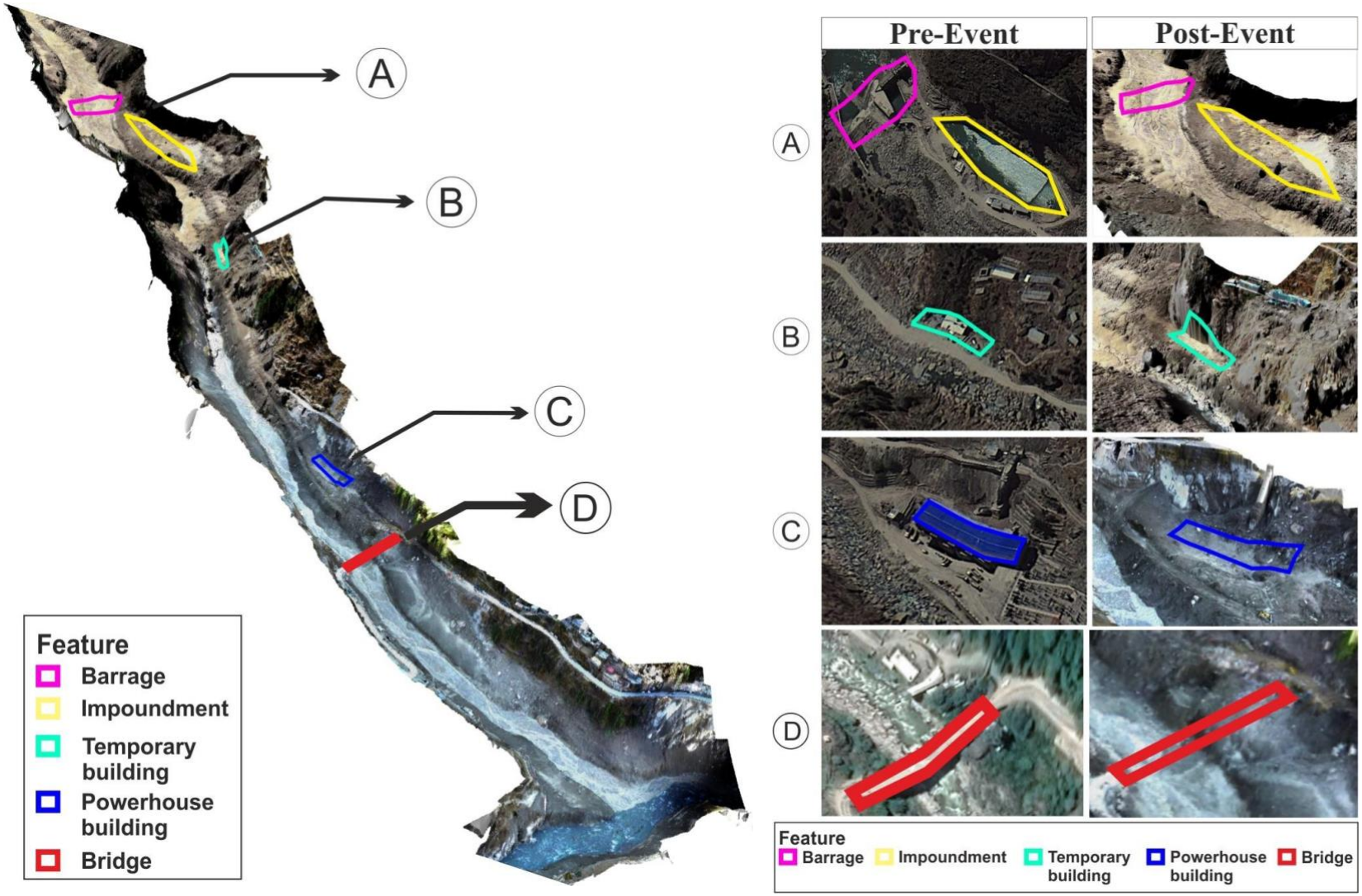

Figure 3.5 3D perspective view of exact locations and the components of the Rishiganga HEP and Raini bridge a) (Left image) mapped in the DEM draped by the mosaic image b) (right image) close-up view of pre (obtained from the Google imagery) and post-event appearance of the infrastructures (Dated: February 11th, 2021) @30°29'5.11"N 79°41'40.46" E

3.1.2 Topography and debris

The pre and post-event DEM valley cross-sections and profiles are utilized to capture the debris flow dynamics and the trend of soil erosion, debris deposition, and break-down of rock fragments.The pre-event DEM is created using the Google Earth, DEM database from GPS Visualizer and ArcGIS. Google Earth is used to locate and obtain a large dataset of point coordinates (longitude and latitude) from the site of interest. GPS Visualizer is used to search for the best possible andaccurate elevation values from the DEM databases such as Shuttle Radar Topography Mission (SRTM, resolution-30m) and Advanced Spaceborne Thermal Emission and Reflection Radiometer(ASTER, resolution-30m). ArcGIS is used to create DEM of the pre-event from the dataset of these points. The post-event DEM is created using the data set generated from the high-resolutiondrone survey.

It may be noted that pre-event DEM is processed by 'Natural Neighbor' or 'area stealing spatial interpolation (Sibson, 1981) in ArcGIS to improve its resolution as close to the post-event DEM. Figures 3.7a and 3.7b present pre and post-event DEMs of the Rishiganga HEP region at 10cmresolution. The locations A, B, C, and D, are also highlighted in Figures 3.7 a and 3.7b for clarity. Although the final resolution of pre-event and post-event DEM are the same, the drone-based post-event DEM is more accurate, while the interpolated pre-event DEM represents the average topography and may include elevation errors. Therefore the quantitative analysis presented in the following sections, despite some errors is helpful for preliminary assessment of topographical changes, flow dynamics, and the tendency of deposition and erosion.

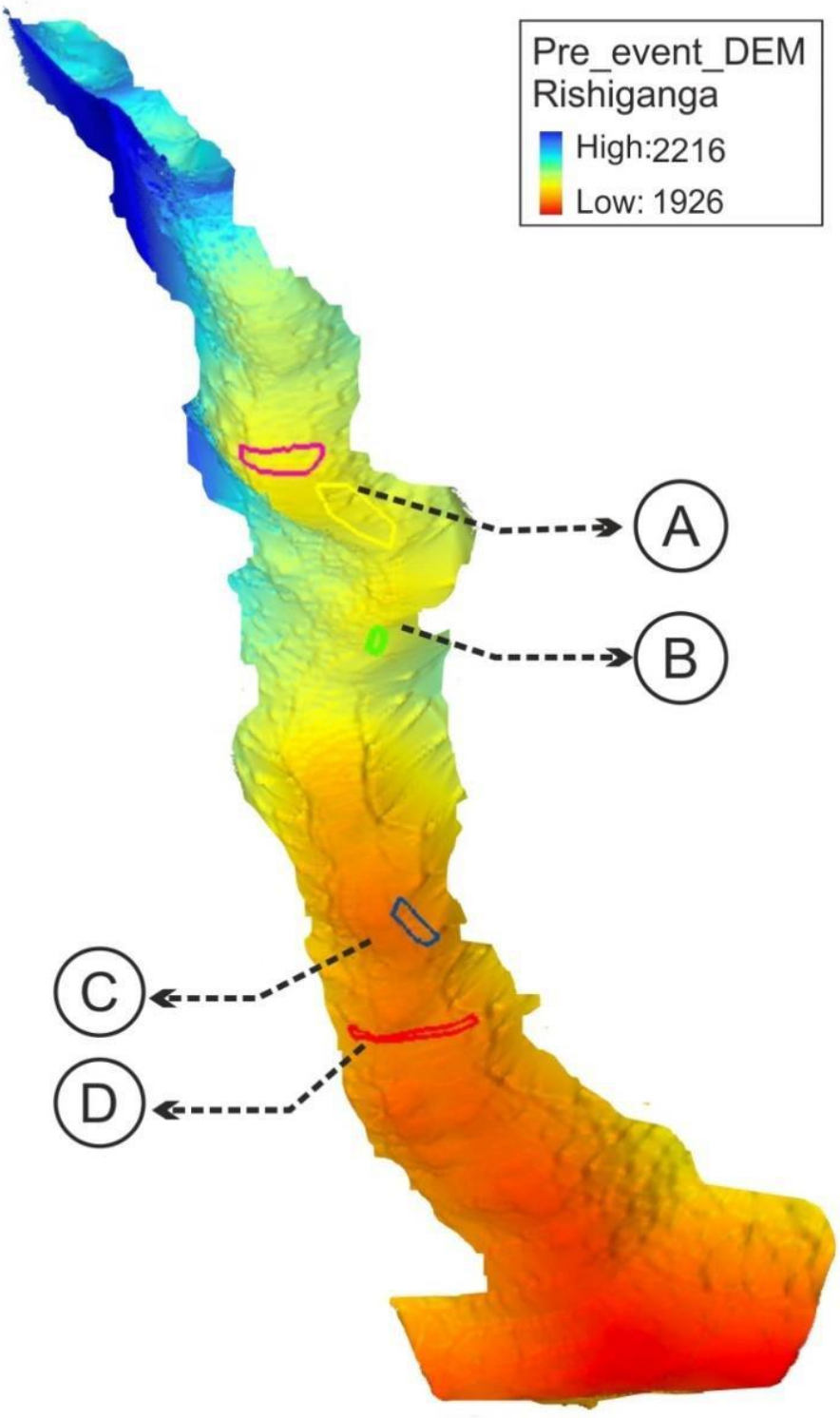

(a)

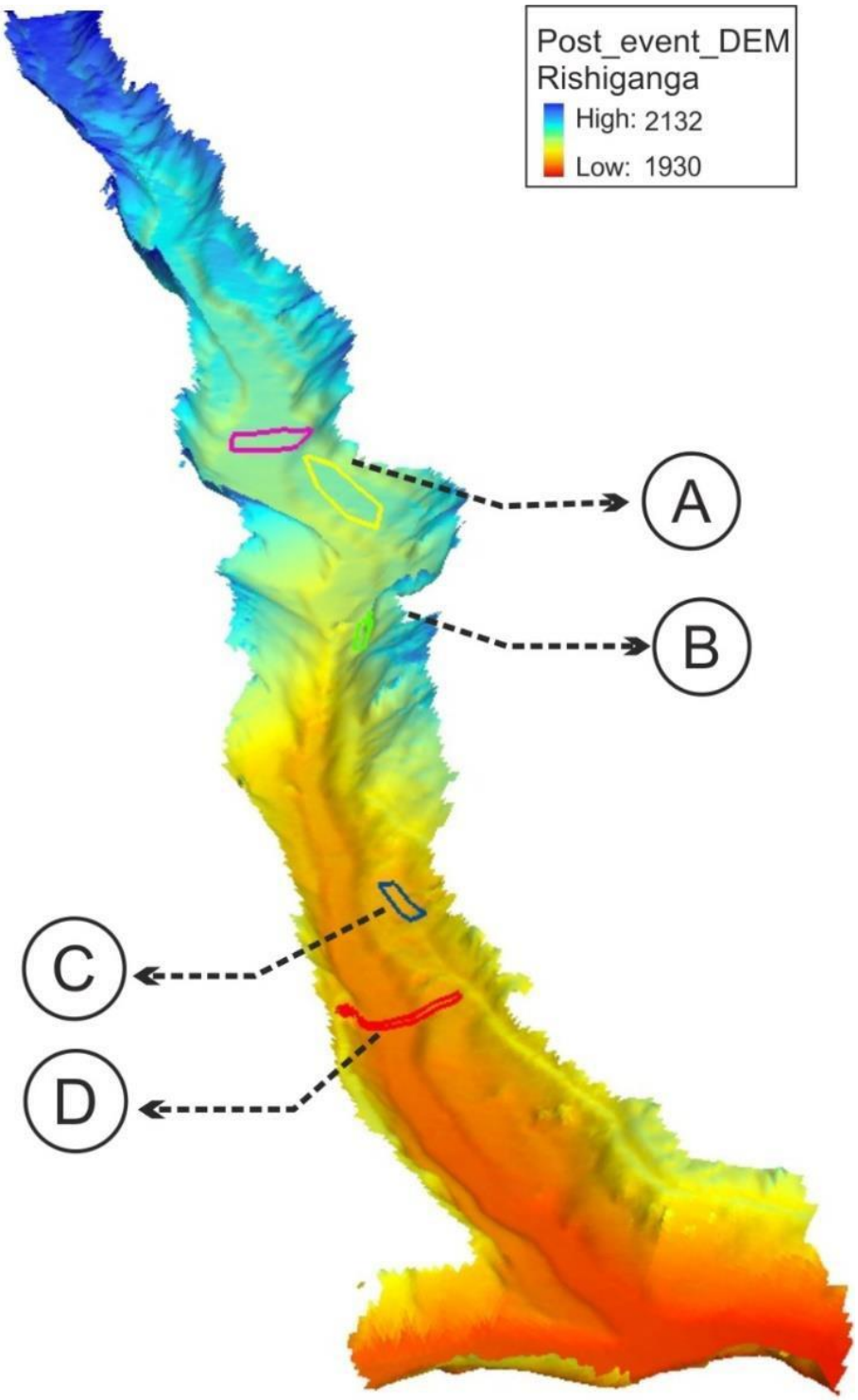

(b)

Figure 3.6 DEMs of Rishiganga area a) pre-event and b) post-event@30°29'5.11"N 79°41'40.46"E

3.1.2.1 Debris flow characteristics based on cross-section and elevation

A total of 13 cross-sections at important locations were examined for pre and post-event to understand the debris flow dynamics. The selected cross-sections are abbreviated as CS# (#1 through 13), as shown in Figure 3.8. CS1 and CS13 represent cross-sections located near upstream of the barrage and the confluence of the rivers, respectively. The barrage is located around CS6, the powerhouse is between CS9 and CS11, and the bridge was at CS11. The elevation profile across cross-sections CS-1 to CS-13 are shown in Figure 3.9, and can significantly influence the flow velocity.

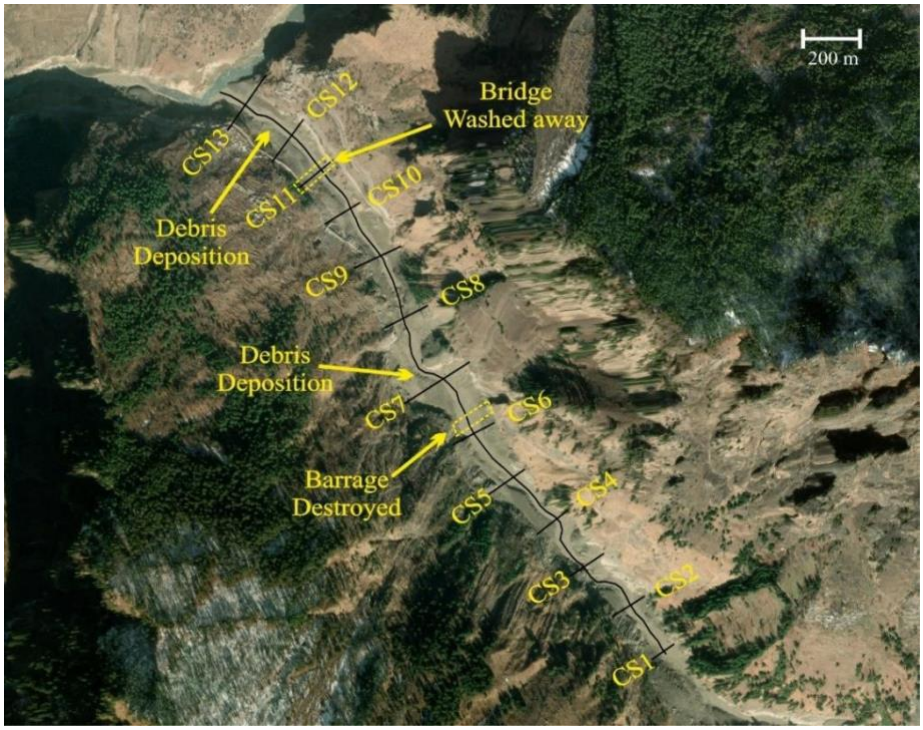

Figure 3.7Proposed cross-sections along the riverbed from CS1 to CS13 from post-event orthophoto and DEM @30°29'5.11"N 79°41'40.46"E

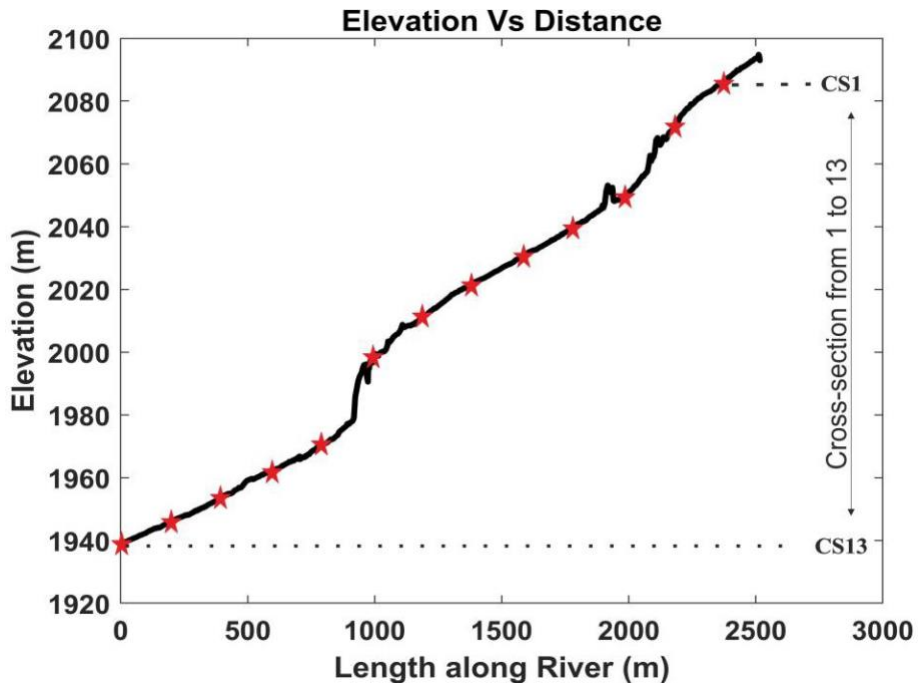

Figure 3.8 Surface elevation profile in the valley along the riverbed from CS-1 to CS-13.

The pre-event and post-event cross-sections were obtained from their respective DEMs. Figures 3.10 and 3.11 compare the pre and post-event cross-section shapes and areas, respectively. The cross-sectional profiles were generated from DEM using the ArcGIS Spatial Analyst tool. Further these profiles were opened in MATLAB to generate the valley cross-sectional area. It can be observed that the shape and area of the post-event cross-sections are due to erosion and debris deposition in the valley. A majority of the erosion can be noticed on the right bank of the valley and deposition on the left side of the bank.

Generally, the broader cross-section of the valley implies a decrease in the flow velocity, causing the flow to lose energy and momentum, leading to debris deposition. In contrast, narrow cross-sections can speed up the debris flow and may result in erosion of the valley. Figure 3.9 clearly shows that area of the pre-event cross-sections varies significantly between CS1 to CS13. The area increases gradually from CS1 to CS6 and followed a rapid increase and sudden drop betweenCS6 and CS8. The CS8 and CS9 cross-section areas are almost identical, and the lowest

area was noticed at CS10. Again gradual increase after CS10 till CS13 can be observed.

Similarly, from Figure 3.9, it is evident that there is a significant change in elevations between the cross-sections from CS1 to CS13; the maximum and minimum are 2090m and 1950m, respectively. A steep decline in elevation and increase in slope is observed between CS8 and CS9. This could have increased the flow velocity, aggravated debris flow's momentum, and caused massive destruction to the nearby powerhouse and bridge. These rapid and sudden changes in cross-sections (shapes and sizes) and elevations explain the extent of damage to the structures due to increased flow velocity and energy. An analysis of the cross-section study revealed the critical flow dynamics and plausible relation to the extent of damage and debris deposition.

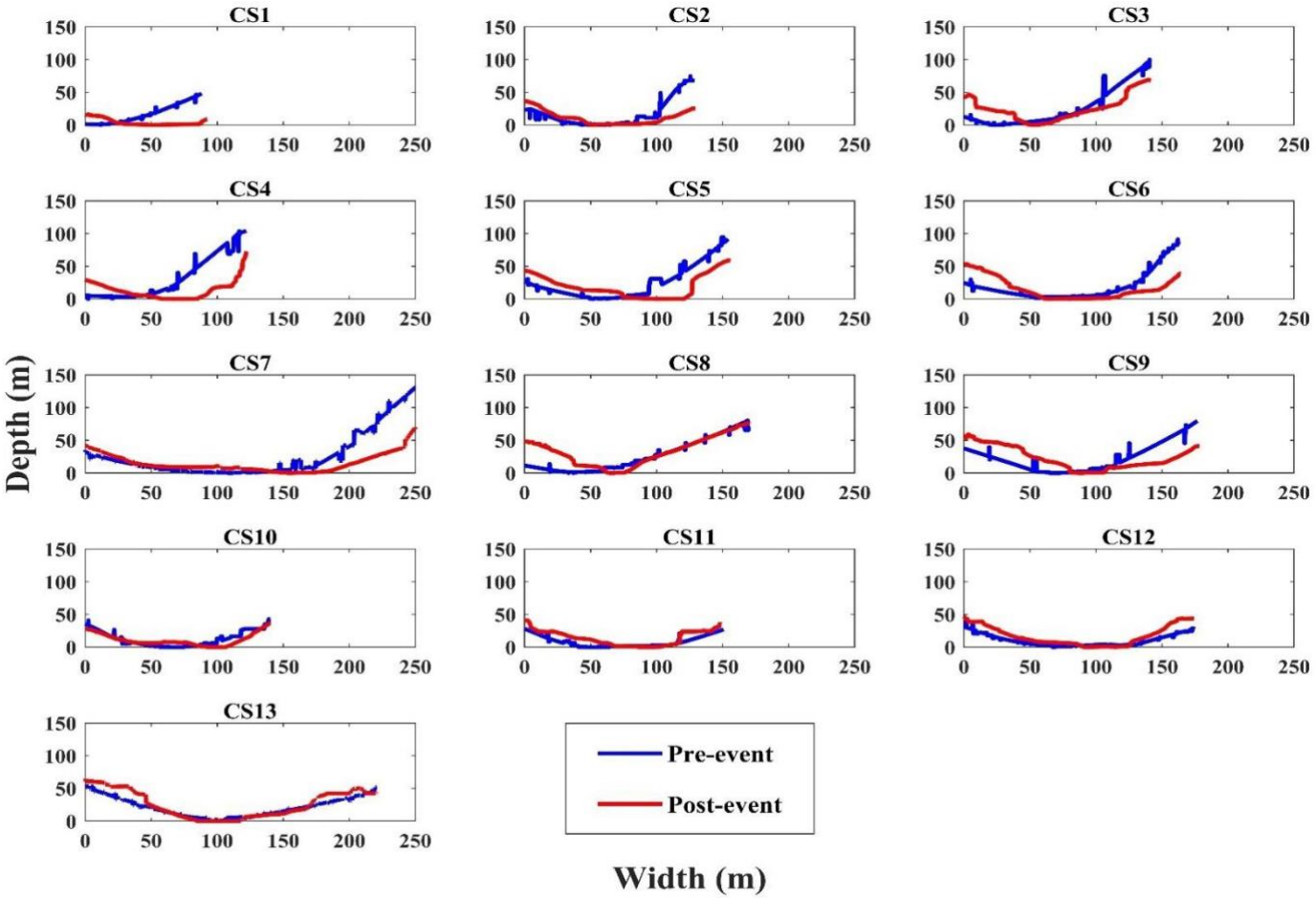

Figure 3.10 Variation of cross-sectional shape in the valley along the river from CS-1 to CS-13.

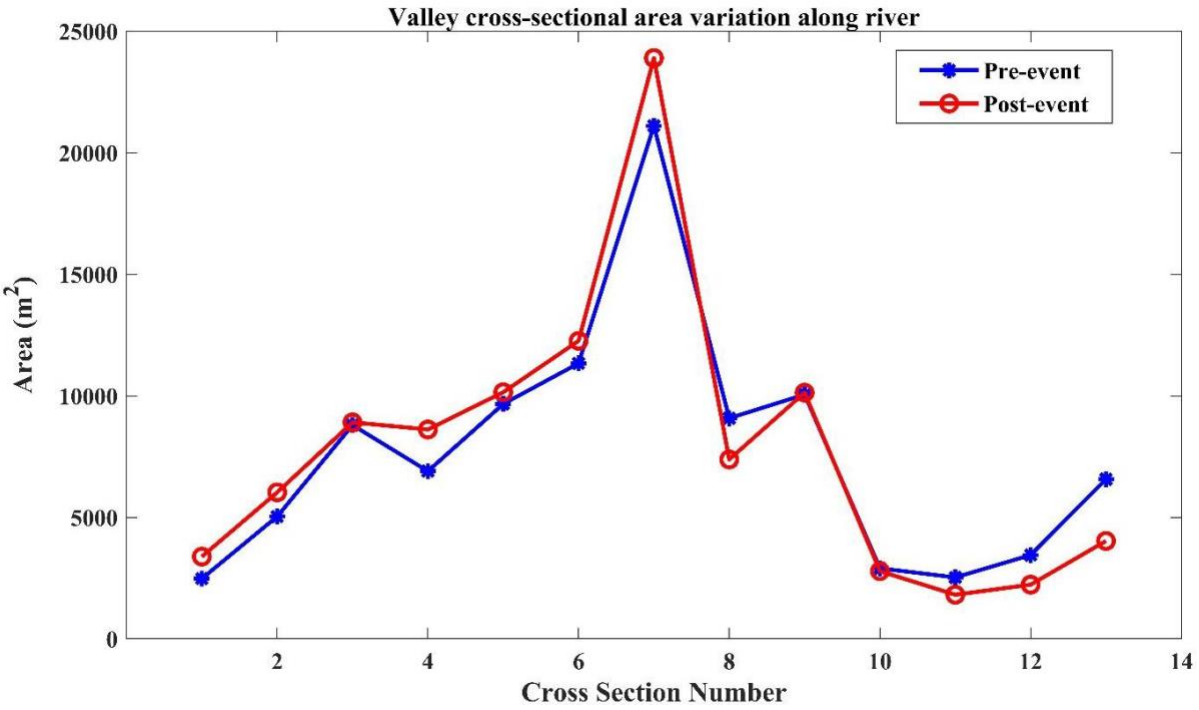

Figure 3.11 Variation of the cross-section area in the valley along the river from CS-1 toCS-13

3.1.2.2 Flood level at Rishiganga-HEP

The visible watermarks left by the debris flow along the Rishiganga river were identified using DEM draped by the mosaic images. The post-event baseline is assumed at the centerline ofthe Rishiganga river flowing in the longitudinal direction (middle of the Rishiganga) observed on February 11th, 2021. The debris flow watermark elevations, baselineelevations, and location of cross-sections are shown in Figure 3.12. Only the debris watermarks selected in the region from CS6 through CS11 are shown, as they were distinctly visible. The maximum and minimum elevations for debris watermark and baseline at CS6 and CS11 are 2090m and 1990m and 2030 m and 1950 m, respectively. The watermark profile is decreasing with the decrease in the elevation from CS-6 to CS-13 as excepted. However, sudden variations in the watermarks are noticed at different locations from CS-6 to CS-13. These variations can be attributed to their valley cross-section shape and area. At Raini bridge (CS-11), the elevation of the debris, watermark rises

despite the increase in the cross-section area of the valley. This increase may be attributed to splashing caused by the obstruction at the Raini bridge and temporary blockage of the flow at the confluence of Rishiganga and Dhauliganga (Figure 3.27). The steep decreasein the cross-sectional area after CS-7 (Figure 3.10) causes an increase in the flow velocity and thewatermark trendline between CS-7 and CS-8 (Figure 3.11). Watermark decreases again after CS-12, which is due to the increase in cross-sectional area.

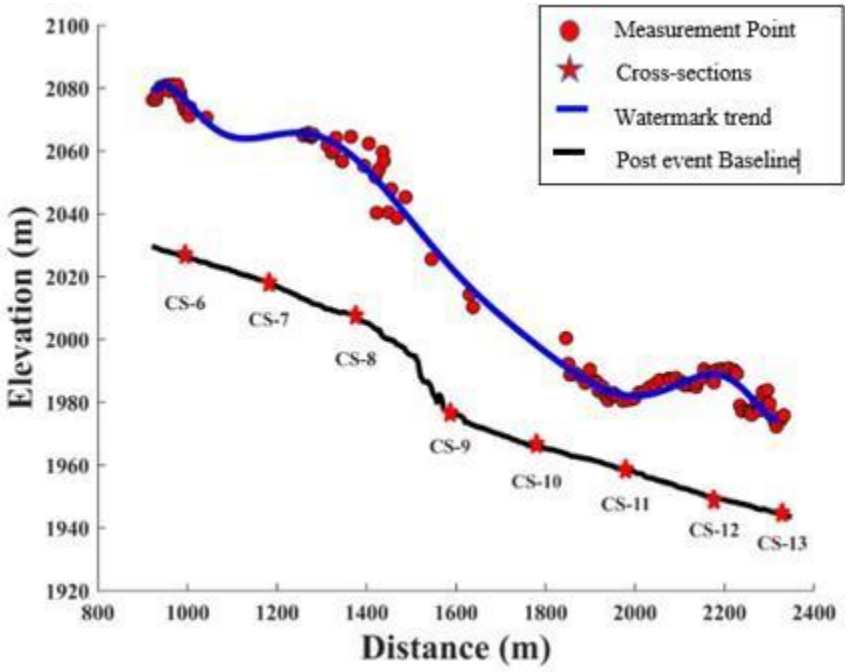

Figure 3.12 Variation of flood watermark along Rishiganga and Raini village

3.1.3 DEM analysis for erosion and debris deposition

The raster image calculation of subtracting pre-event DEM (Figure 3.7a) from post-event DEM (Figure 3.7b) produced a new raster image, often addressed as DEM of Difference (DOD), as shown in Figure 3.13. The pixels of the DOD raster image include positive and negative elevation values (in meters) representing deposition and erosion, respectively. The red and blue shaded zones are used to distinguish the positive and negative elevations, as shown in Figure 3.13. It can be

observed that the majority of the right bank of the valley is in the blue shade, indicating debris deposition consistent with observations deduced from the pre and post-event cross-section analysis. It is also evident from Figure 3.13 that the infrastructure at locations A, B, and C got buried by the debris deposition, as is also evident in Figures 3.1b, 3.5, and 3.6. Significant erosion is observed at the location just above A and B, and moderate erosion along the valley center portion and left bank. The bridge location C experienced both erosion and deposition.

The shape and size of the cross-sections, and their elevations, as well as the built infrastructure, significantly influenced erosion and debris deposition patterns. For instance, a gradual increase of cross-sectional area is observed between CS-10 to CS-12, causing debris deposition in these areas. The increase in cross-sectional area from CS-6 to CS-7 is abrupt but decreases afterward. This sudden increase in the area reduces the increased flow velocity through CS-6 and deposits massive debris at CS-7 just after eradicating the barrage and side slopes of the valley.

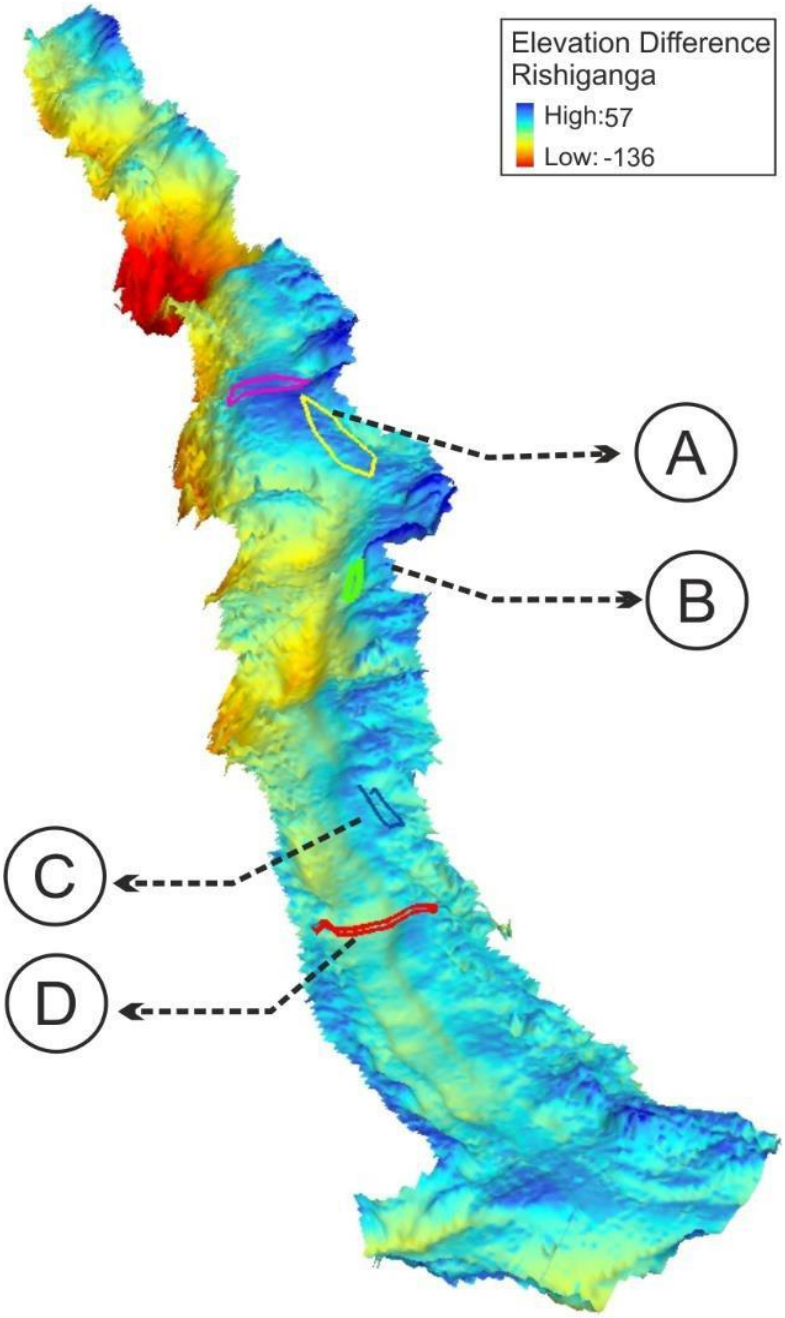

Figure 3.13 DEM of difference between pre-event and post-event DEM of Rishiganga HEP@30°29'5.11"N 79°41'40.46" E

3.1.3.1 Slope and Curvature Changes

To further understand the effect of debris flow on the valley, the slope and curvatures of the valley have been examined by estimating these parameters using ArcGIS. The rate of elevation change for each digital elevation model (DEM) cell is represented by a slope. Slope values are estimated from the post-event DEM (resolution-1m) of Rishiganga using ArcGIS and categorized in nine different classes from 0 to 90 degrees (Figure 3.14). The locations "A-D" in Figure 3.12b have a slope between 0-10 degrees after the debris deposition. The analysis shows that slope values were minimal in the observed impact zone, indicating that the terrain has flattened, which may be due to the erosion and subsequent deposition of debris. The curvature values (second derivative of the surface) are calculated from the post-event DEM (resolution-1m) of Rishiganga using ArcGIS. The curvature function displays the shape or curvature of the slope, which can be concave, convex, or flat (Figure 3.15). Figure 3.16 shows more than 75% of the coverage area in blue shades that have positive curvature values indicating that the surface is upwardly convex. This might be due to the debris deposition and signifies a tendency for accelerated flow and erosion. The zone near the bank of Rishiganga shows negative curvature values indicating that the surface is upwardly concave. This might be due to the cutting and eroding of the valley due to the debris flow and now tends to decelerate flow and deposition. (Figure 3.16).

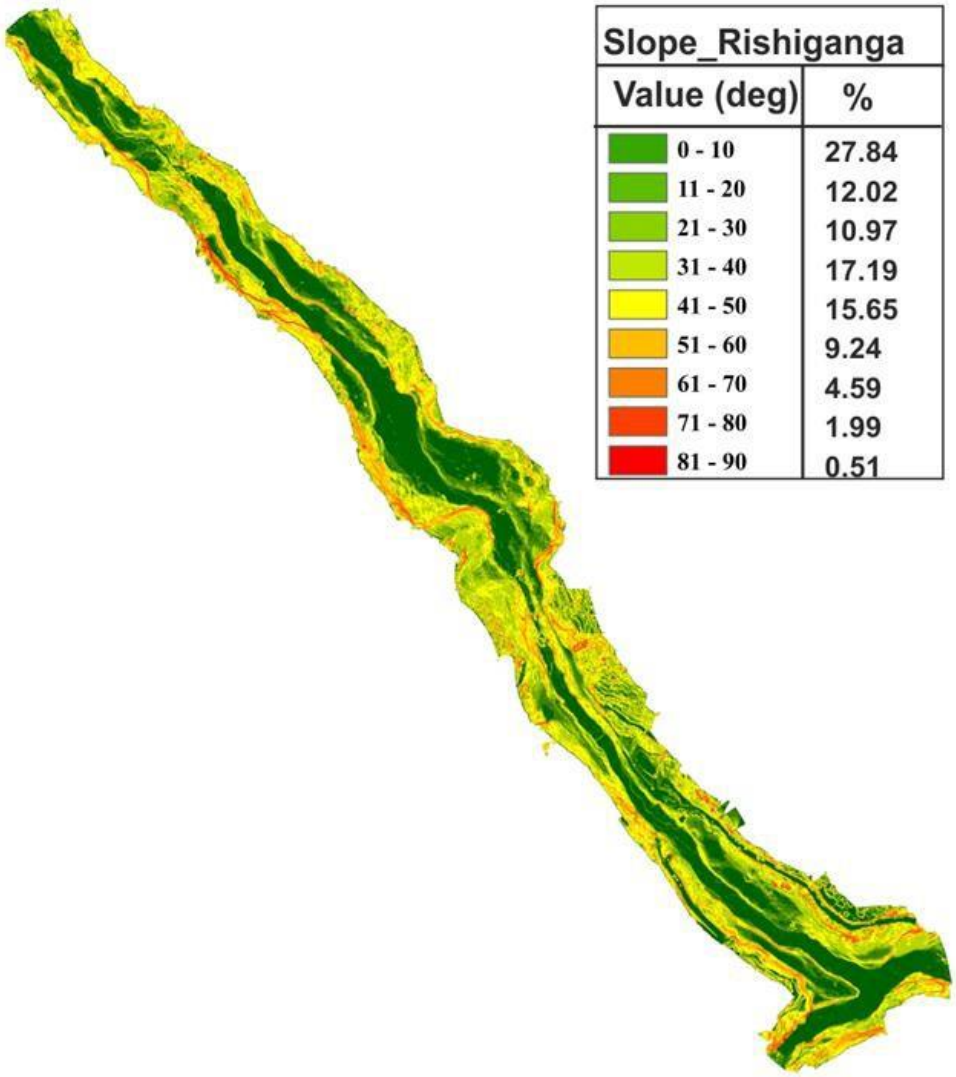

Figure 3.14 Slope calculated from DEM (resolution-1m) of Rishiganga HEP@30°29'5.11"N 79°41'40.46"E

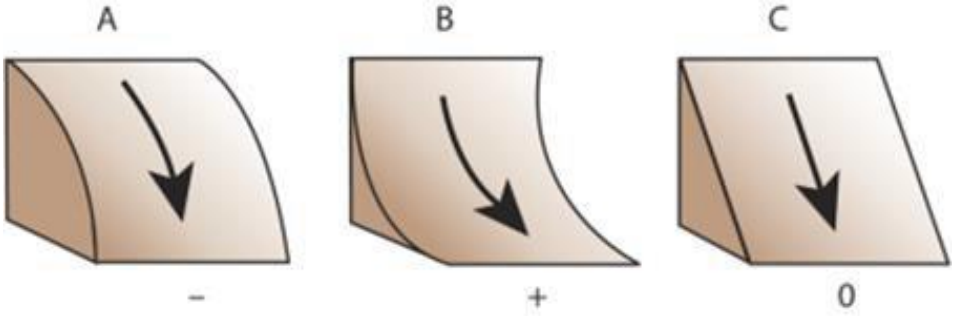

Figure 3.15 Types of profile curvature (ESRI ArcGIS manual)

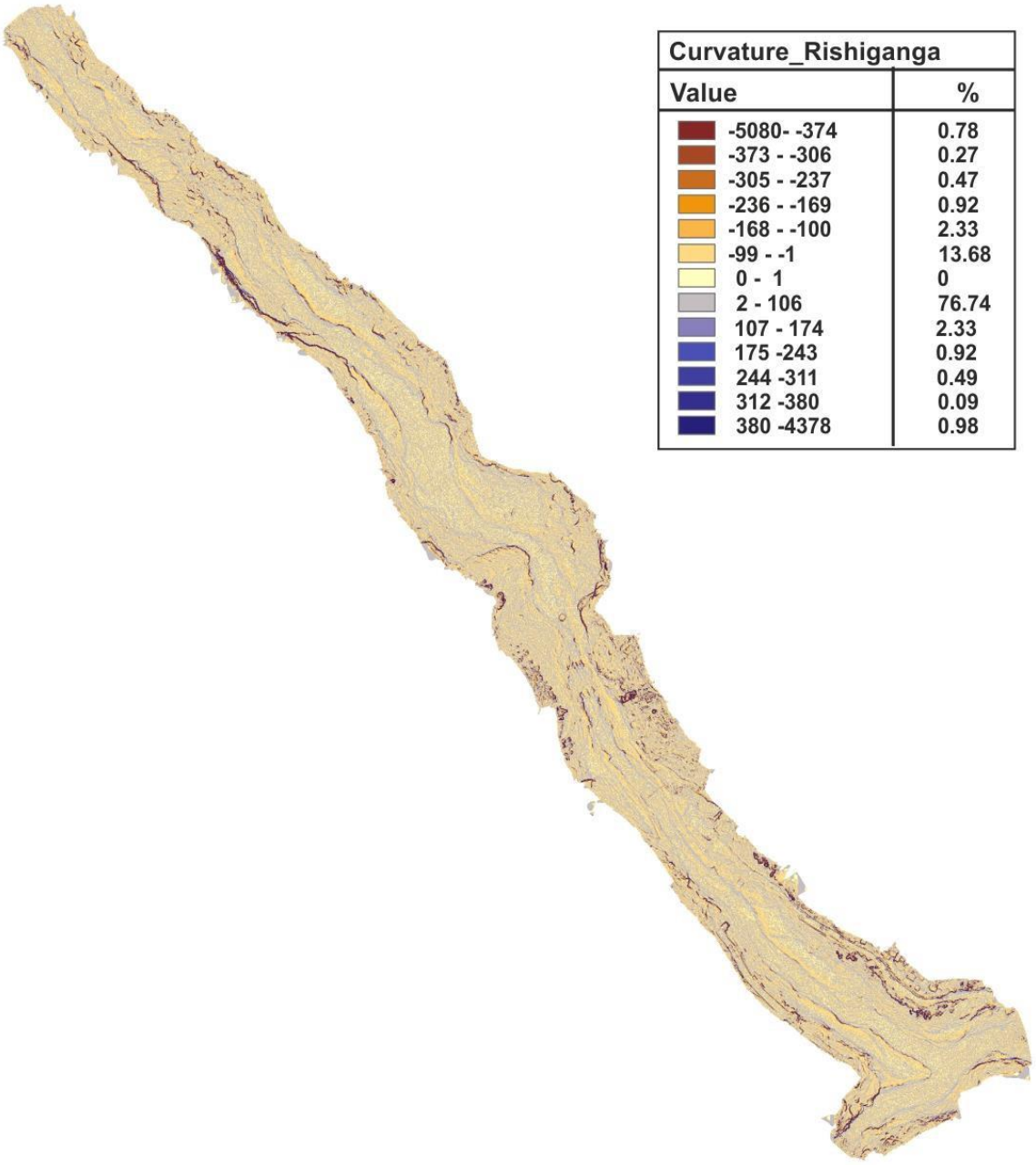

Figure 3.16 Profile curvature calculated from DEM (resolution-1m) of Rishiganga HEP @30°29'5.11"N 79°41'40.46"E

3.1.4 Photogrammetry evidence of Studied area - I

The valley floors upstream and downstream of the Rishiganga HEP were heavily deposited by debris consisting of soil, broken pieces of infrastructures, and fragmented rocks of mountain sides collected from the source and along the pathway of flash floods. Figures 3.17-3.19 present the upstream and downstream valleys of R-HEP show the muddy depositions (consisting of sediment grains ranging from 75µm to 2 mm, as obtained from the sieve analysis performed on the samples brought from the site) and boulders of sizes ranging from 0.5 m to 5 m.

3.1.4.1 Barrage and Impoundment (A)

The barrage of the powerhouse was partially washed away and partially submerged under the debris, as shown in Figure 3.17. Similarly, damage to the other supporting structures such as water impounding and intake zone for the headrace tunnel was exceptionally severe, as shown in Figures3.18 - 3.20.

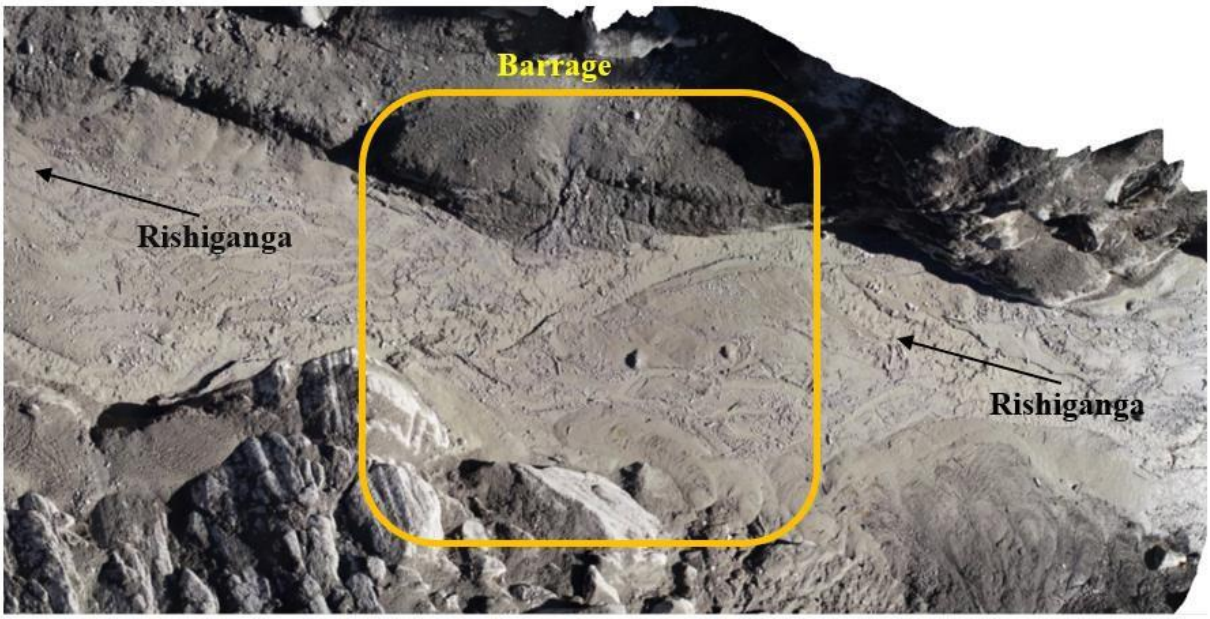

Figure 3.17 Barrage region, 30°28'42.68"N 79°42'0.50" E (Dated: 11/2/2021)

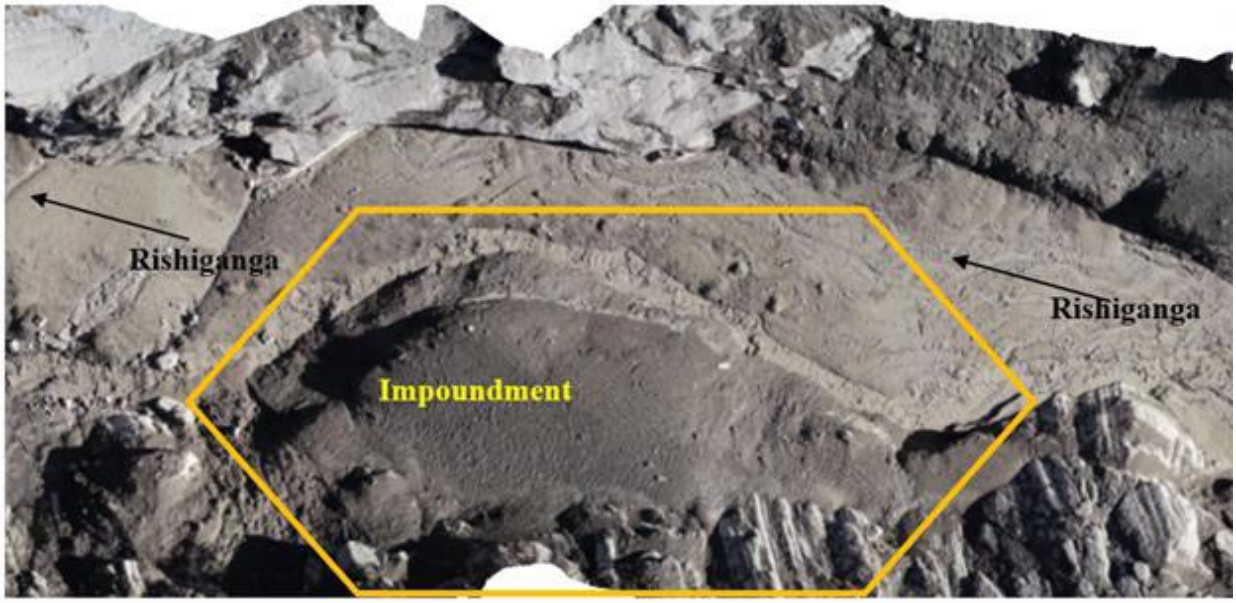

Figure 3.18 Marks of impoundment region@ 30°28'45.39"N 79°41'53.46" E (Dated:11/02/2021

Figure 3.19 Accumulated Boulders/ Broken concrete structures, a few centimeters ahead ofthe tail of impoundment @ 30°28'47.40"N 79°41'53.25"E (Dated:11/02/2021)

Figure 3.20 Buried pipe/tunnel structure@ 30°28'56.39"N 79°41'49.20" E

3.1.4.2 Temporary buildings (B)

Figure 3.21a shows the pre-event imagery of November 17th, 2018 obtained from Google Earth. This image highlights the temporary buildings near the downstream of the barrage, whereas 3.21b gives a post-event close-up view of the same location, filled with debris and giant boulders.

a)

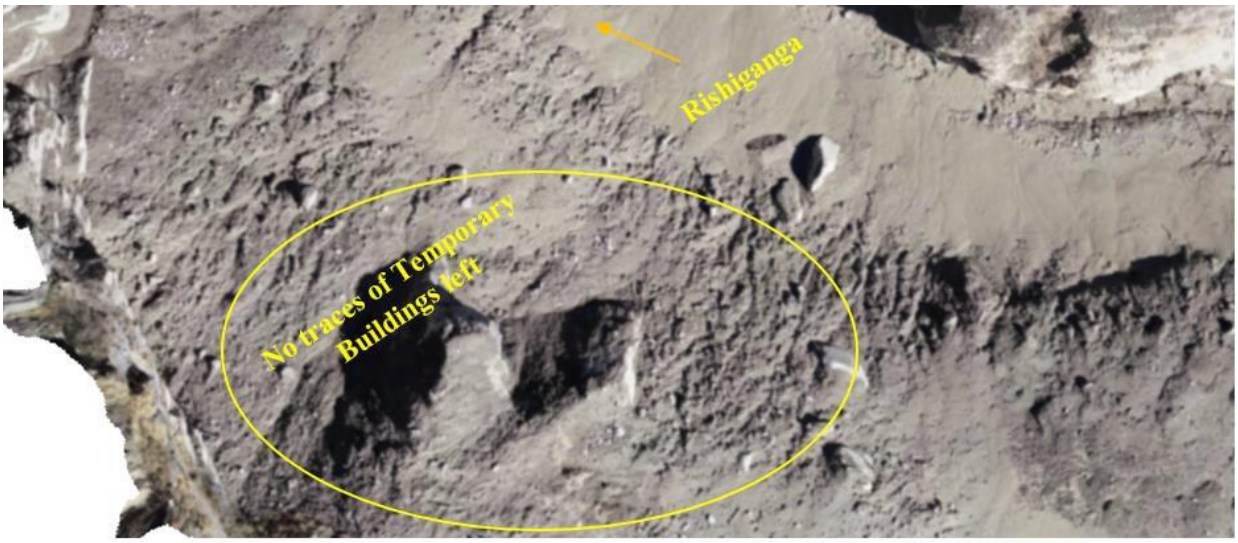

b)

Figure 3.21 a)Pre- and b) Post-event temporary building location @ 30°28'46.26"N 79°41'50.83"E (Dated:11/02/2021)

3.1.4.3 Powerhouse (C)

The powerhouse site also experienced similar damage. Figures 3.22 and 3.23 show thatthe multi-story building, powerhouse, and utility structures were washed away from their locations. The extent of the damage caused by the flash flood at the penstock location can be seen clearly in the images in Figure 3.24. The debris mark (solid red line), as shown in Figure 3.24a, indicates the height the flood reached up to the of the penstock, which is at an elevation of about 1986 m MSL, causing damage to the penstock support system (steel bars are exposed) and burying the turbine with debris.

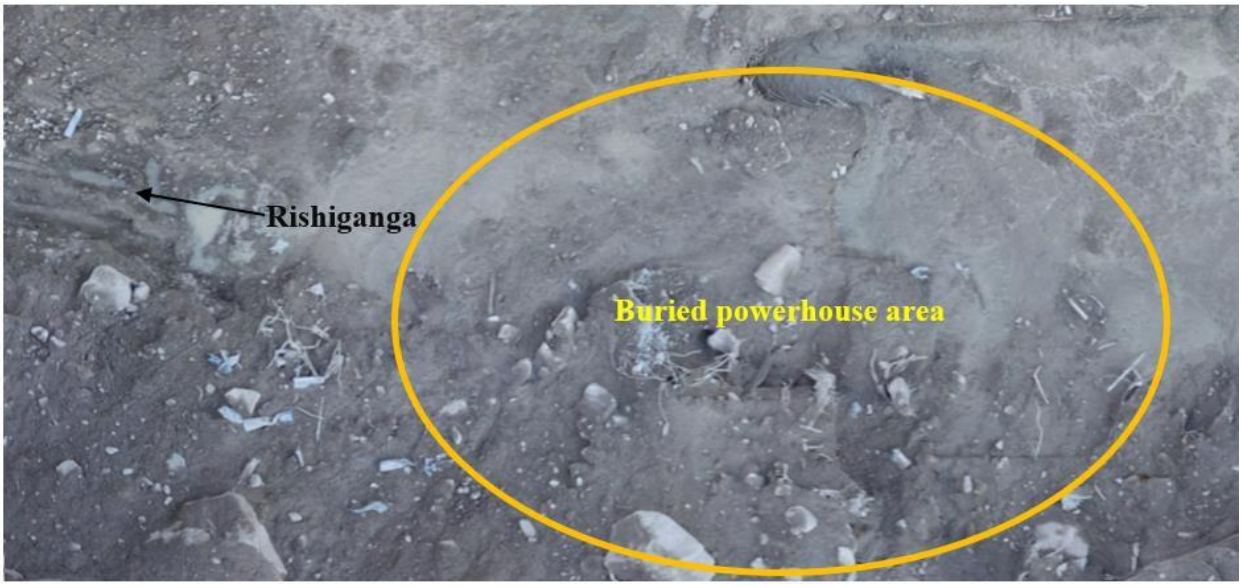

Figure 3.22 Buried powerhouse region @30°29'5.11"N 79°41'40.46" E (Dated: 11/02/2021)

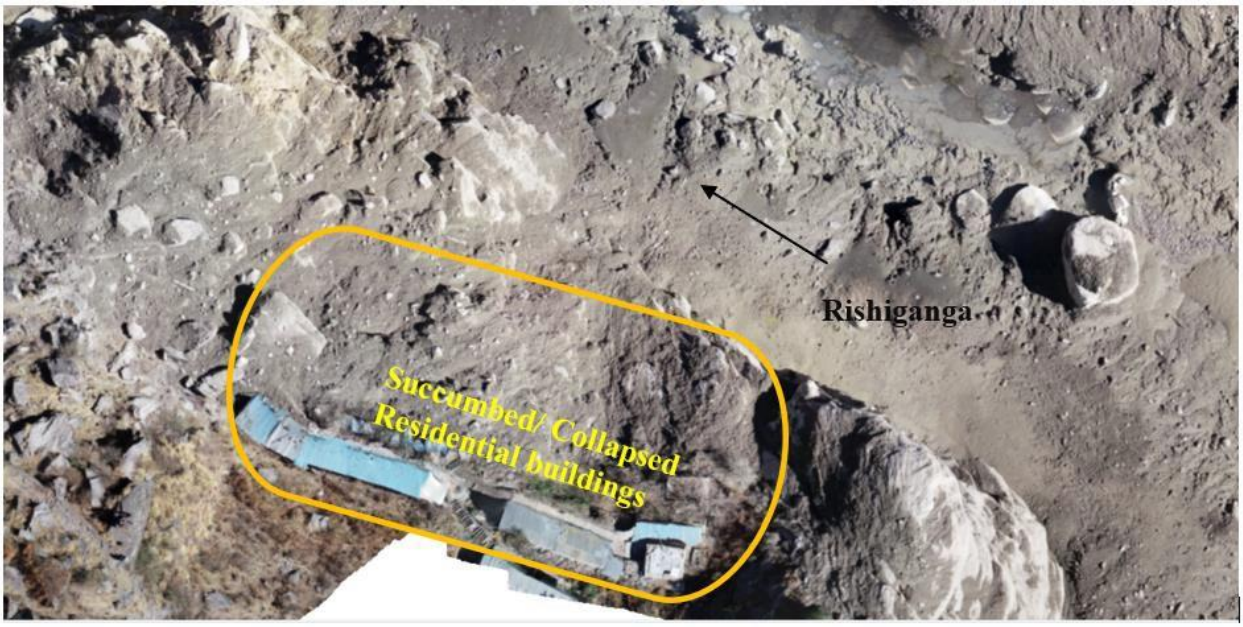

Figure 3.23 Damaged/Buried Residential Houses@ 30°28'51.83"N 79°41'49.93"E(Dated: 11/02/2021)

(a)

(b)

Figure 3.24 Post-event images at the location of the penstock illustrate the damage caused, exposed reinforcement, and deposition of debris covering the penstock a) top view (30°29'2.57"N 79°41'40.91"E) b) side view. (Dated: February 11th, 2021)

3.1.4.4 RCC Bridge (D)

The right bank abutment and the approach slab of the RCC bridge were severely damaged and buried under the muddy deposits, in contrast to the left bank abutment and approaching slab, as shown in Figure 3.25. It also clearly shows the bridge superstructure at an elevation of 1973 MSL was completely washed away by flash floods.

Figure 3.25 Damaged Raini bridge across the bank of Rishiganga River with only leftabutment and no decks. (30°29'7.95"N, 79°41'39.56"E) (Dated: February 11th, 2021)

3.1.4.5 The confluence of Dhauliganga and Rishiganga

The debris flow moving with extremely high velocity and kinetic energy crashed with the mountain face at the Dhauliganga and Rishiganga confluence and formed craters on the face, as shown in Figure 3.26 in solid black lines. The mountain on the right bank of Dhauliganga acted like a barrier in the path of incoming massive debris flow from Rishiganga and created a temporary blockage. It resembles the "water hammer" phenomenon in the dam when gates behind penstocks are closed abruptly. The temporary blockage at the confluence resulted in impounding and raising the water level upstream of the Dhauliganga, evident from the debris mark highlighted in the solid blue line in Figure 3.27.

Figure 3.26 Crater formation at mountain face from the collision of debris flow with thehill (N30°29'11.30", E79°41'29.65", Elevation-1989 m). (Dated: February 11th, 2021)

Figure 3.27 Raised watermarks upstream of Dhauliganga as proof of temporary blockageof the main river and debris throwback after the impact with the hill. (N 30°29'11.30" E079°41'29.65", Elevation-1989 m) (Dated: February 11th, 2021)

3.2 Study Area – II: Tapovan HEP

The tragic episode of flash floods in Chamoli has led to infrastructure damage in and around Tapovan-HEP as well, which was under construction. The catchment area of this project is3,100 square kilometers. Naithani and Murthy, 2006, reported that Tapovan Dam consists of hydropower related structures such as a desilting basin (140m (L) ×76.5m (W)), an intake structure with four bays each of 8.0 m width and separated by 1.5 m thick piers with 2.8 m high gates, conduits, and barrages with bays of 12m width, each separated by 2.5 m wide piers. This area also consists of breast walls that were constructed to support the piers or hold the water up to a head 12 m above the crest level of the intake, two suspension bridges, i.e., one on the upstream and one on the downstream sides of the barrage, respectively, and a workshop consisting of a batching plant in the nearby vicinityupstream of the barrage on the left bank of the river. Figure 3.28 gives a close-up view of the under-construction barrage site. The NTPC officials took the image on December 14th, 2020 i.e., approximately two months before the extreme event.

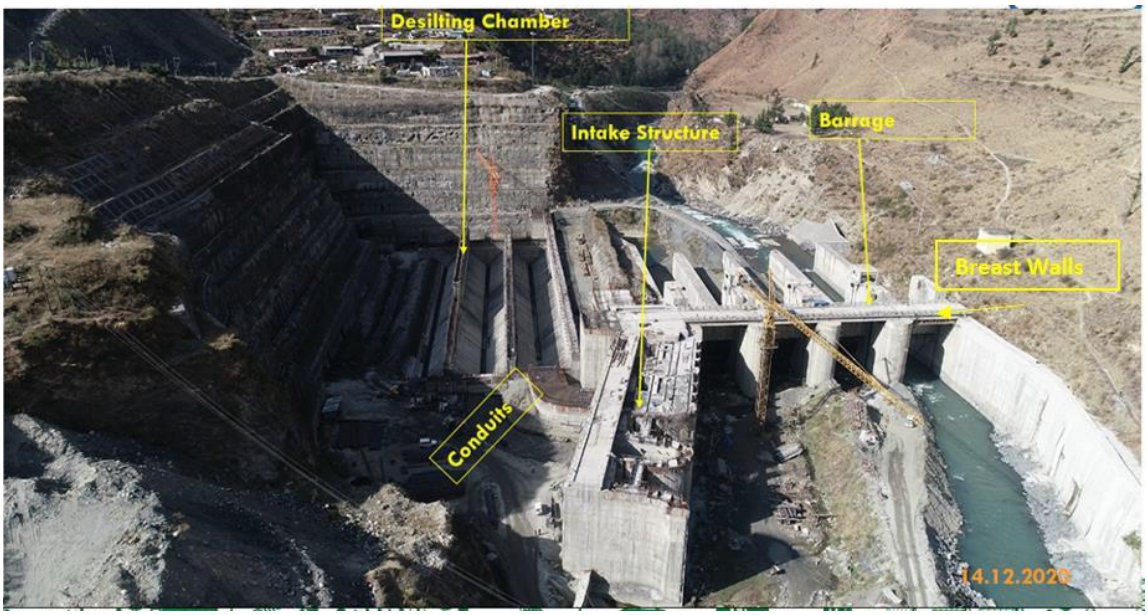

Figure 3.28 Close-up view of barrage site infrastructure (Source: NTPC Tapovan via National Institute of Disaster Management (NIDM), MHA-Webinar on Lessons from Chamoli Disaster 2021 https://www.youtube.com/watch?v=fE6yjZE6pUq&t=1709s) @ 30°32'7.84"N 79°31'10.71" E

The pre and post-event visuals of the TV-HEP are presented in Figures 3.29a and 3.29b, respectively. The pre-event visual was obtained from the Google imagery of 2017, and the post-event was a digital ortho mosaic generated from the drone survey. It is evident from these figures that Tapovan HEP was severely affected by the flash floods and heavily deposited with debris, including soil and boulders of different sizes.

a)

b)

Figure 3.29 Tapovan HEP area (a) pre and (b) post-event orthophoto data showing the collapsed bridges, damaged structures, accumulated boulders, muddy water and, affected barrage gates@ 30°32'7.84"N 79°31'10.71" E

3.2.1 Photogrammetry evidence of TV-HEP

A post-event drone-based reconnaissance study similar to Rishiganga HEP was conducted at the affected TV-HEP site to visualize and document the damage caused by the flash flood. The entire data of this site captured by the drone survey was aligned by aerial triangulation. Further, the aligned data was orthorectified and geo-referenced using the GCP information obtained from EMLID RS2 DGPS equipment. Subsequently, the contour lines were generated on a scale of 1:1000. Figure 3.30 clearly shows the contour drawing draped over the orthoimage of TV-HEP. The contours, namely of pink and yellow colors, represent the major and minor contours at an interval of 5 m and 1 m, respectively. The irregular contour lines indicate the uneven surface, whereas closely spaced lines represent steep terrain. The minimum and maximum contour traced by the drone survey are 1840 m and 1905 m. Also, from the generated surface profile, the observed lowest point of the river is noted at 1851 m. The bridge-1, which was upstream of the barrage site, was estimated to be about 117.70 m in length and 7.95 m wide at a height of approximately 20 m from bedrock, and got washed away entirely, as marked by the black color line plotted in Figure 3.30 for reference.

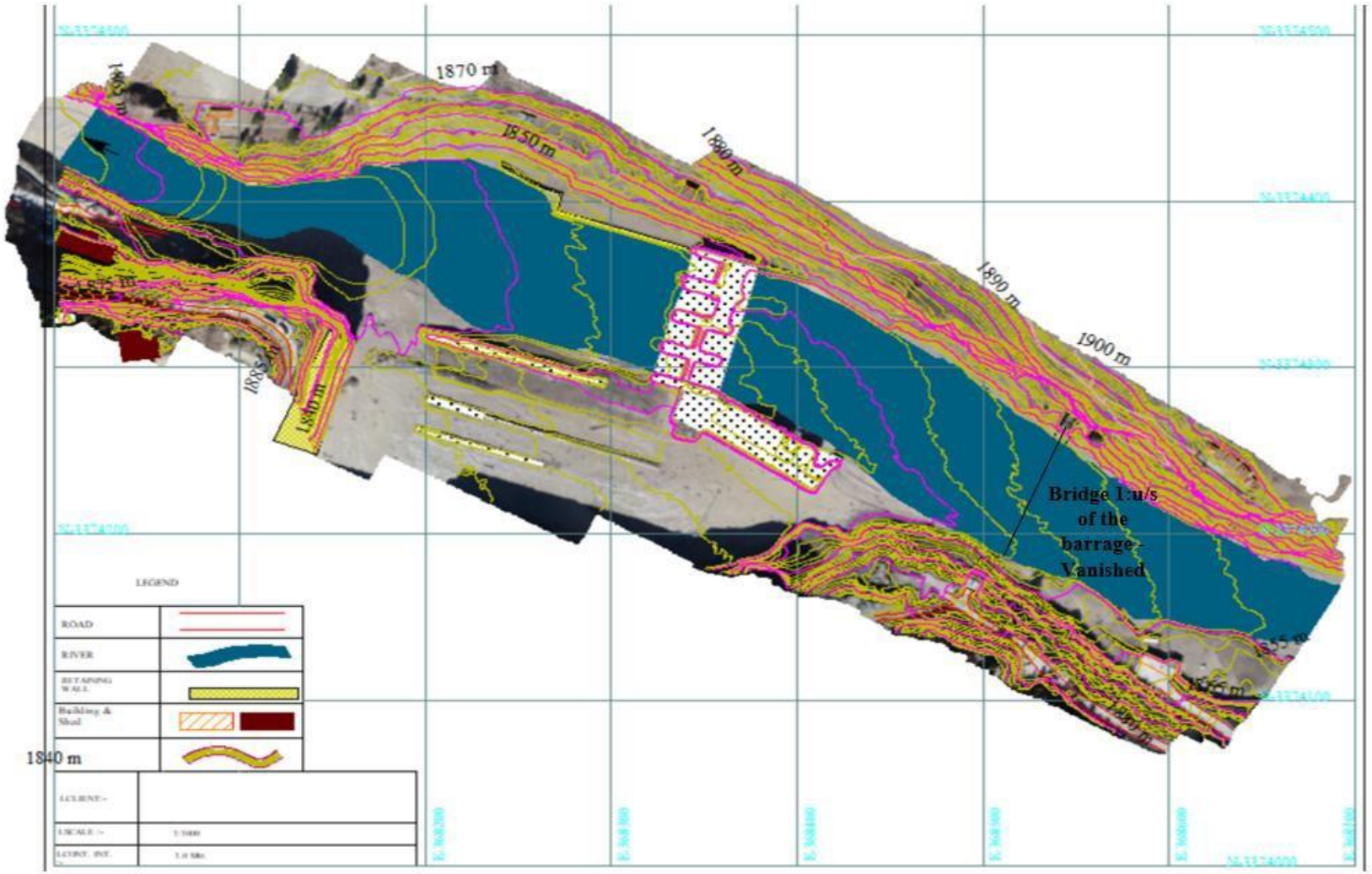

Figure 3.30 Surface plan overlaid on orthophoto @ 30°32'7.84"N 79°31'10.71" E

3.2.2 Flood level at Tapovan-HEP

Figure 3.31a illustrates the ortho mosaic draped over the surface profile of DEM, which is used for identifying the watermarks left by the debris flow at Tapovan HEP. A reference point (X) and an endpoint (Y) were considered at the upstream and downstream line along the selected post-event baseline to obtain the variation of flood watermarks along the scanned area. The points obtained in this region are plotted against the traverse length of the flood, as shown in Figure 3.31b for further analysis. The post-event baseline is assumed at the centerline of the Rishiganga observed on February 11th, 2021. The dotted line in Figure 3.31b represents the deck level of the barrage at an elevation of about 1861m MSL, which is considered the datum point for establishing the high flood level at different elevations. The trend line (solid blue) of the data in the graph clearly shows the debris mark along the valley of the Tapovan-HEP. It's evident from the figure that the difference between the baseline and the debris mark is decreasing from the upstream and downstream reference points X and Y, respectively. However, the elevation difference increased suddenly after the X reference about 100 m (upstream) due to the narrow valley cross-section. It reached a height equal to the barrage about 1864 m MSL including bridge-I and collapsed the bridge and severely affected the barrage.

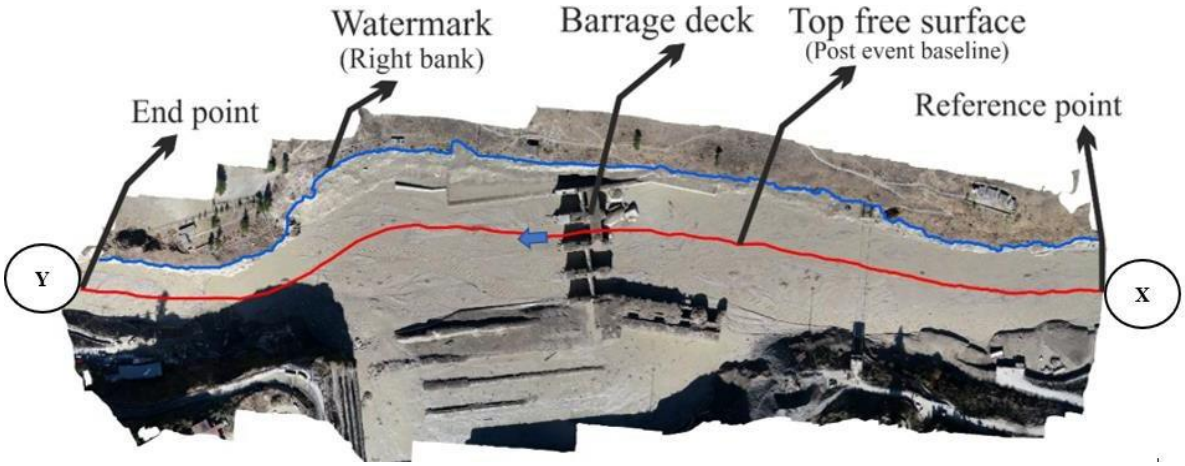

(a)

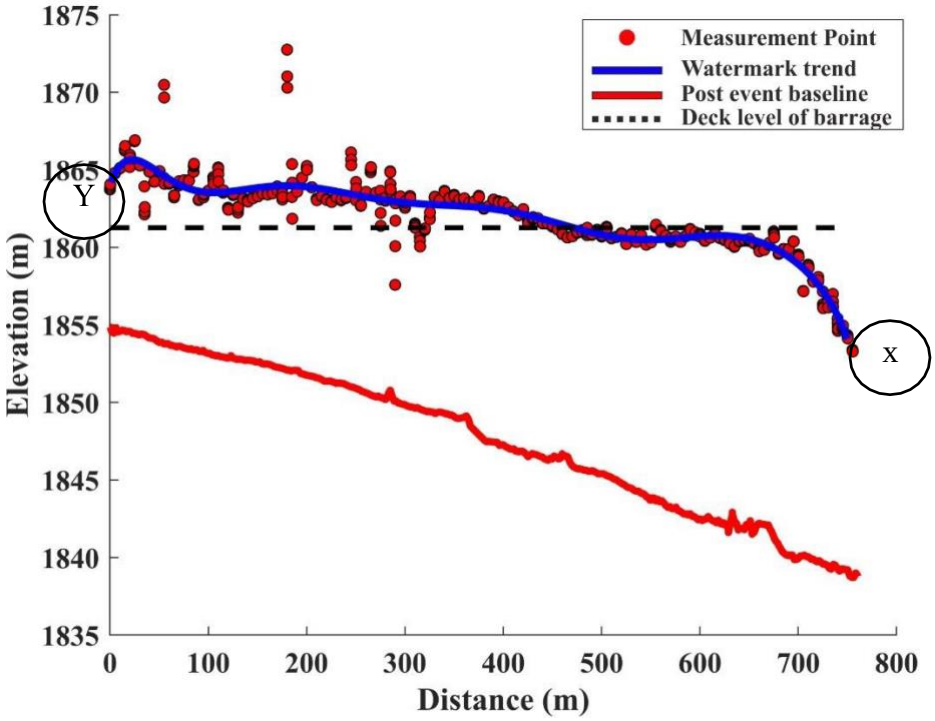

(b)

Figure 3.31 Variation of flood debris marks along the study area a) Orthorectifiedmosaic image b) elevation of debris marks vs. the traverse distance of flood @ 30°32'7.84"N 79°31'10.71" E

3.2.3 3D View of TV-HEP

The post-event aerial view of the entire scanned area of TV- HEP in three dimensions was reconstructed using an ortho mosaic and DEM, as shown in Figure 3.32. The ortho mosaic is draped over the DEM to follow the surface profiles and provide a clear visual understanding of the post-event topography and the conditions of the prominent features at the site.In particular, the barrage, intake structure, and desilting chamber are marked as A, upstream bridge-1, the workshop area is highlighted and marked as B, and bridge-2 in the downstream is marked as C. Figure 3.33 presents the close-up 3D view of these prominent structures (A, B, and C) before and after the event, showing the extent of damage to these structures. The pre-event and post-event 3D views were obtained from the Google Earth imagery and ortho mosaic draped DEM, respectively. The finer details of each feature's damage and ground conditions are discussed with the help of high-resolution geotagged images in the subsequent sections.

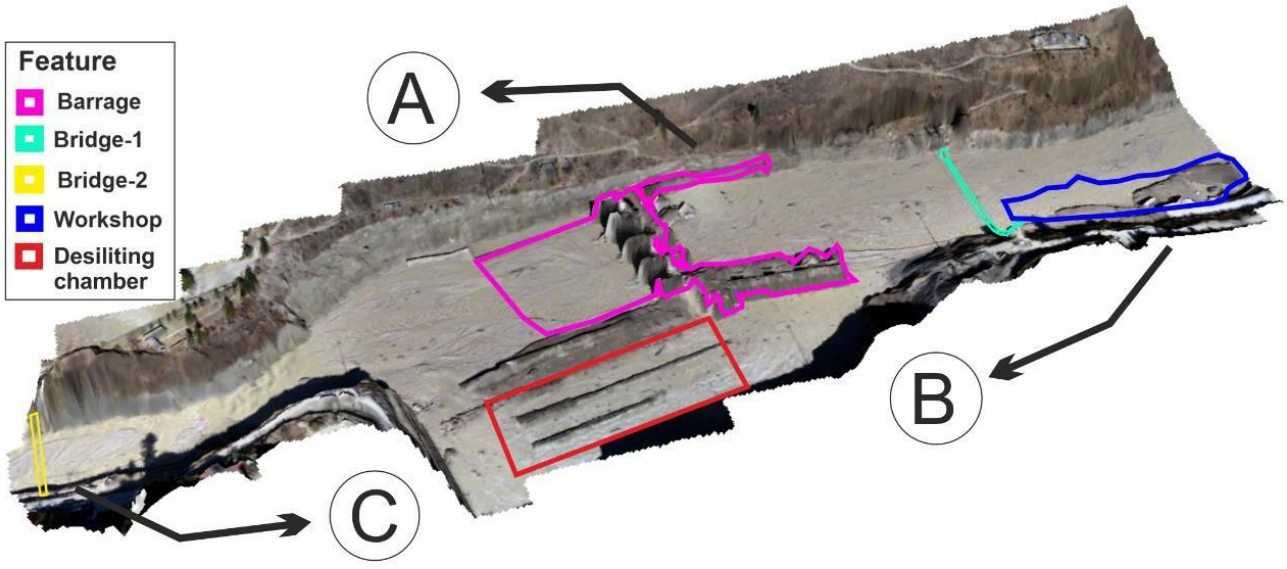

Figure 3.32 3D view of Tapovan barrage site@ 30°32'7.84"N 79°31'10.71" E

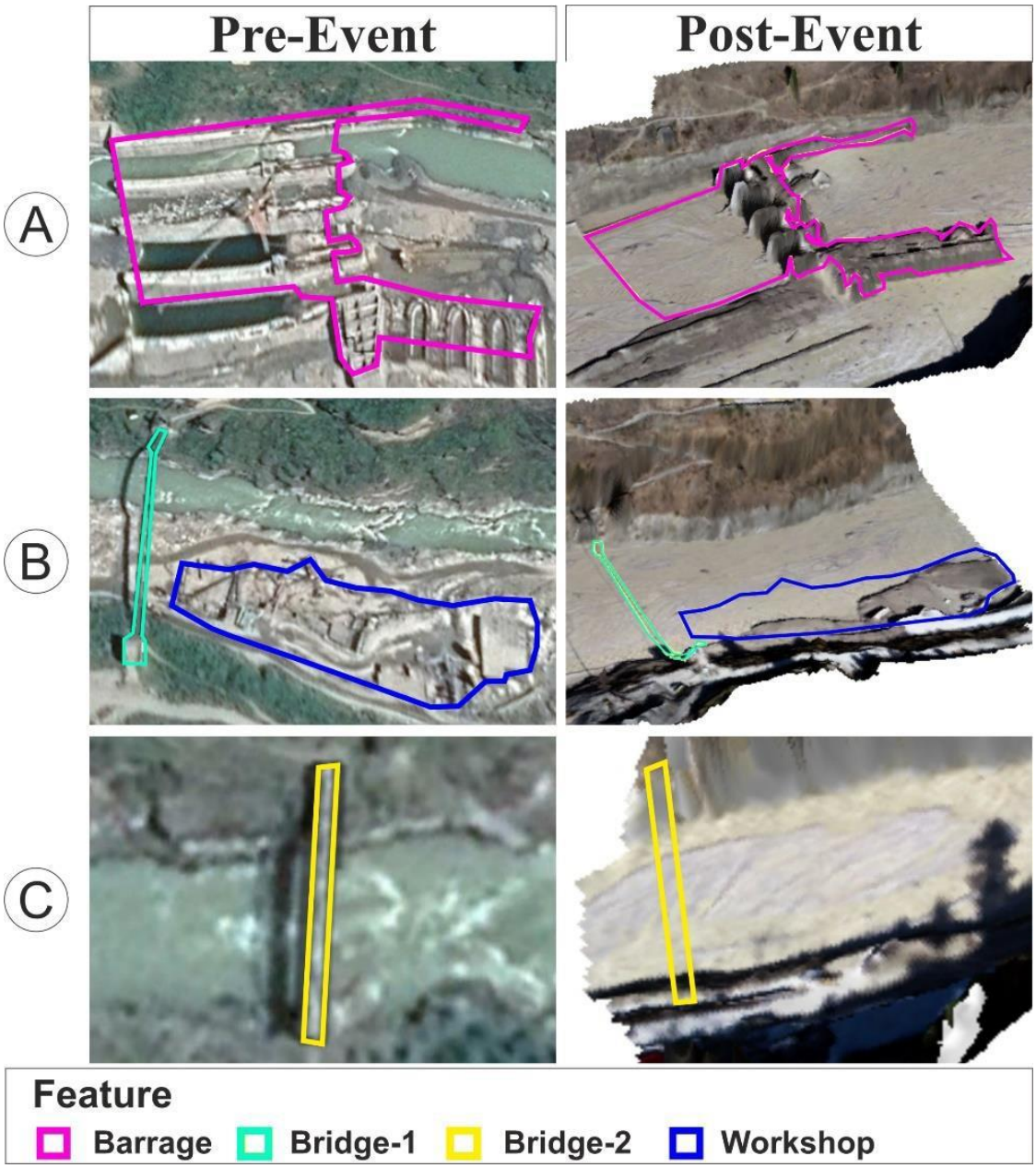

Figure 3.33 Pre-and post-disaster situation at the barrage site. @ 30°32'7.84"N 79°31'10.71" E

3.2.3.1 Barrage site (A)

The piers of the barrage and intake structures suffered massive damage, and large debris deposits were observed over them. The conduits and the desilting chamber, as shown in Figure 3.28, are missing in Figure 3.34, *and are* probably buried by the debris deposition. Figure 3.35 shows a detailed view of the damaged intake structure with a visible layer of deposits, whereas, Figure 3.36 shows the broken and exposed steel bars at the tail of the intake structure (downstream of barrage).

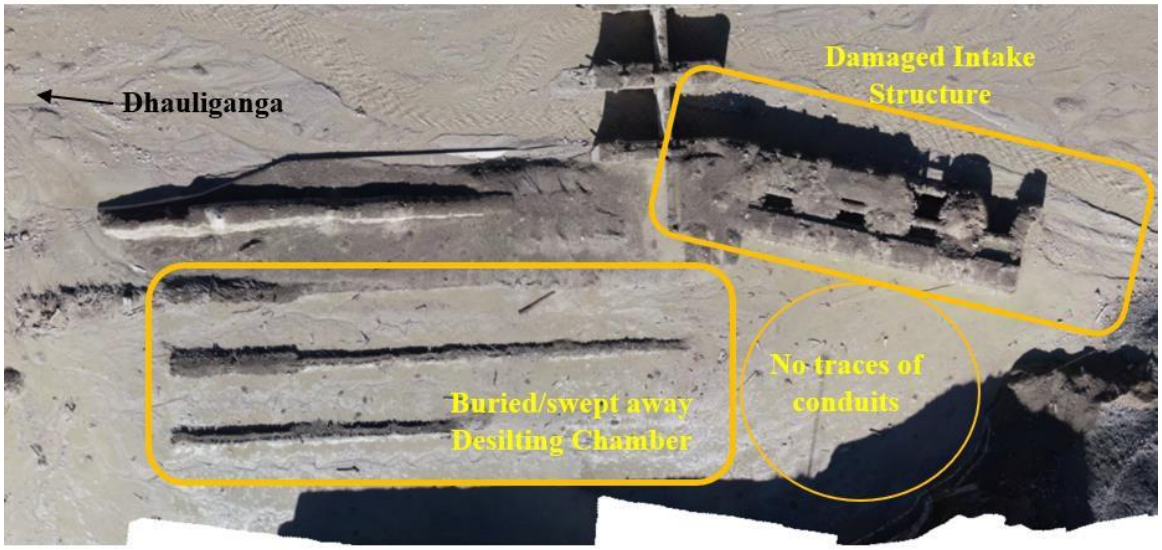

Figure 3.34 Aftermath marks of the Intake structure, desilting chamber, and conduits@ 30°29'35.89"N 79°37'41.67"E (Dated:11/02/2021)

Figure 3.35 Close-up view of the Intake structure@ 30°29'35.89"N 79°37'41.67"E (Dated:11/02/2021)

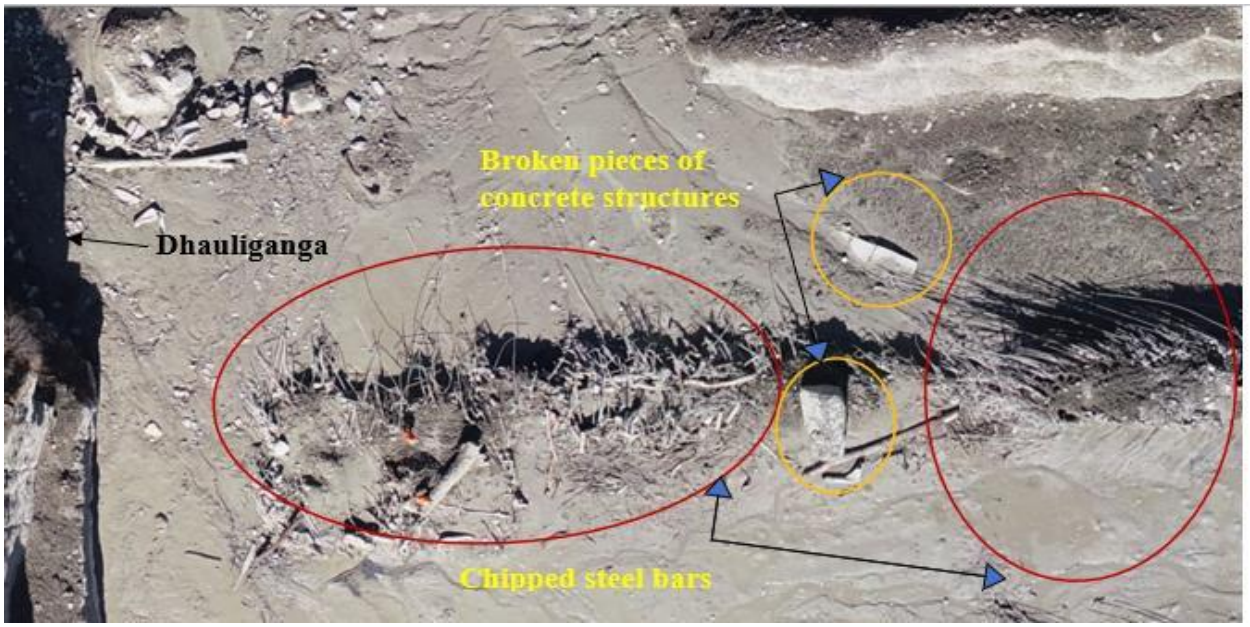

Figure 3.36 Distorted steel bars at the tail of intake structure @ 30°29'35.89"N 79°37'41.67"E (Dated:11/02/2021)

Almost half of the breast wall over the barrage top was washed away, as shown in Figure 3.37. Huge boulders of different sizes were carried by the floods are retained by the piers of the barrage, as illustrated in Figure 3.37.

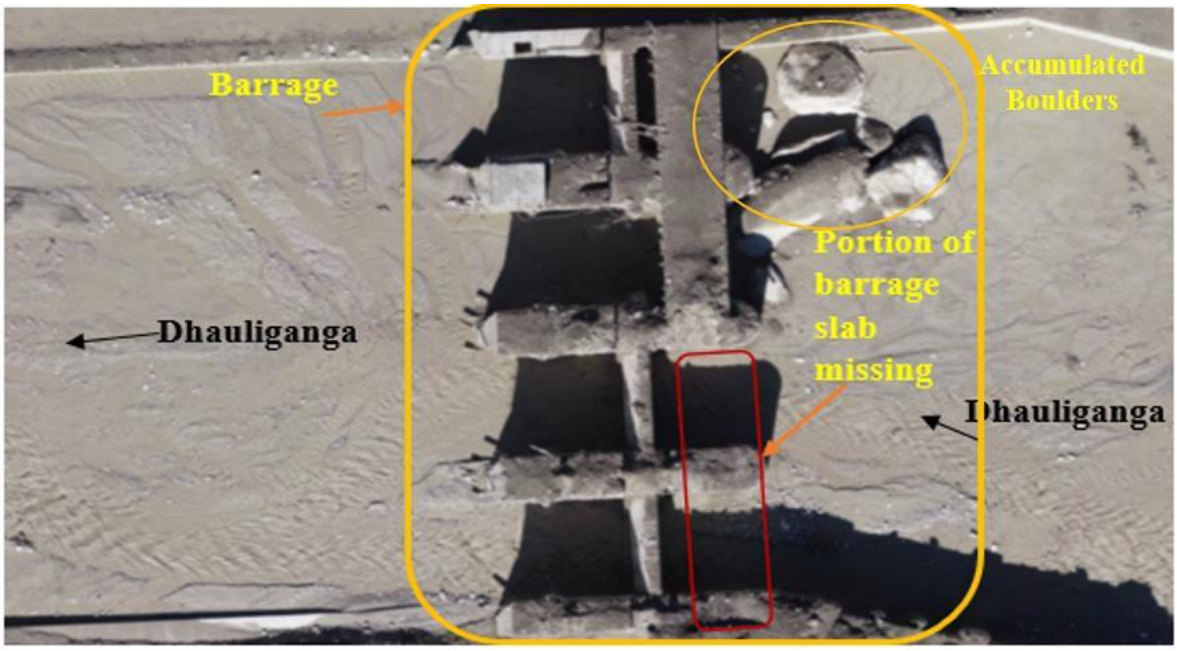

Figure 3.37 View of Tapovan barrage @ 30°29'35.89"N 79°37'41.67"E (Dated:11/02/2021)

The post-event orthophoto and Global Mapper were used to estimate the dimensions of the damaged barrage, breast walls, and the boulders behind the barrage piers. The total length of the breast wall over the barrage before the event was about 83 m long, whereas post-event, about 41 m length of this breast wall had been washed away, as shown in Figure 3.38. The approximate length of the boulders came out 10.2 m and 19.6 m which is $1/8^{th}$ and $1/4^{th}$ of the calculated total length of the breast wall, which indicates that the flow velocity must have been sufficiently high, which led to the accumulation of huge boulders near the gates.

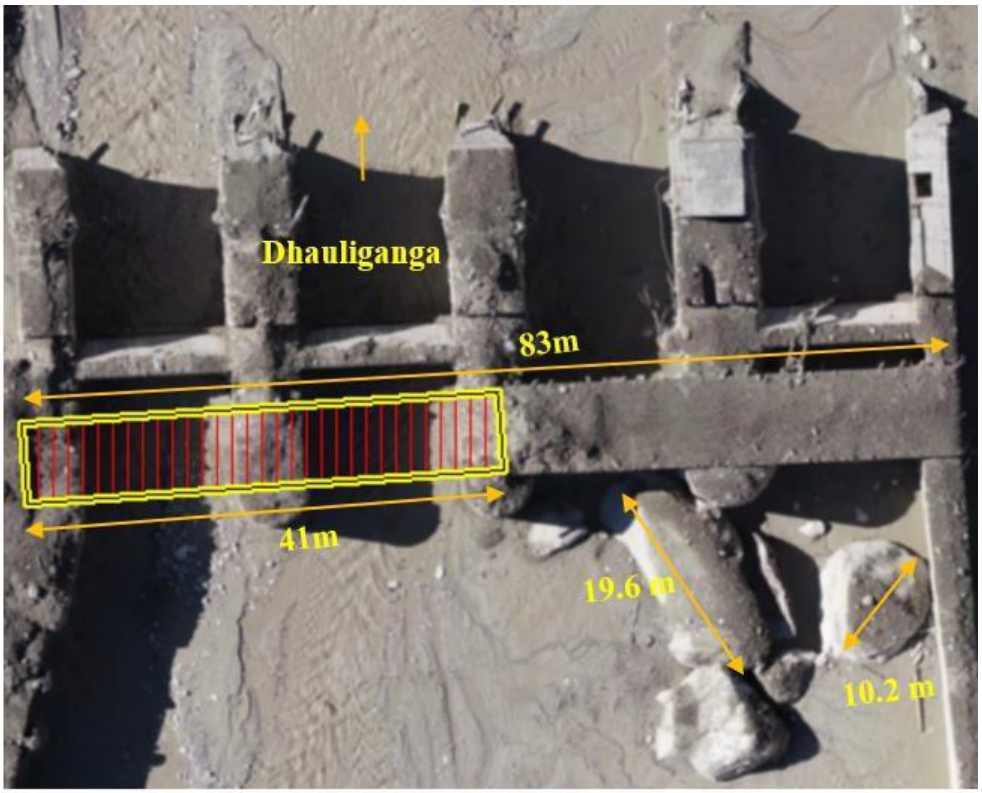

Figure 3.38 Dimensions of the existing and vanished portion of the breast wall(highlighted with red strips) along with the accumulated boulders. @ 30°29'35.89"N 79°37'41.67"E (Dated:11/02/2021)

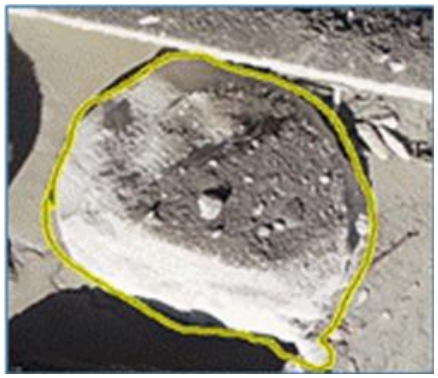

Figure 3.39 Close-up view of a boulder@ 30°29'35.89"N 79°37'41.67"E (Dated:11/02/2021)

Figure 3.40 presents the status of guard/operation rooms constructed on top of the barrage.Figure 3.40a shows that the flood has reached to top level of the barrage piers to reach the guardroom during the event and wash away one of the guardrooms, as shown in Figure 3.40b.

(a)

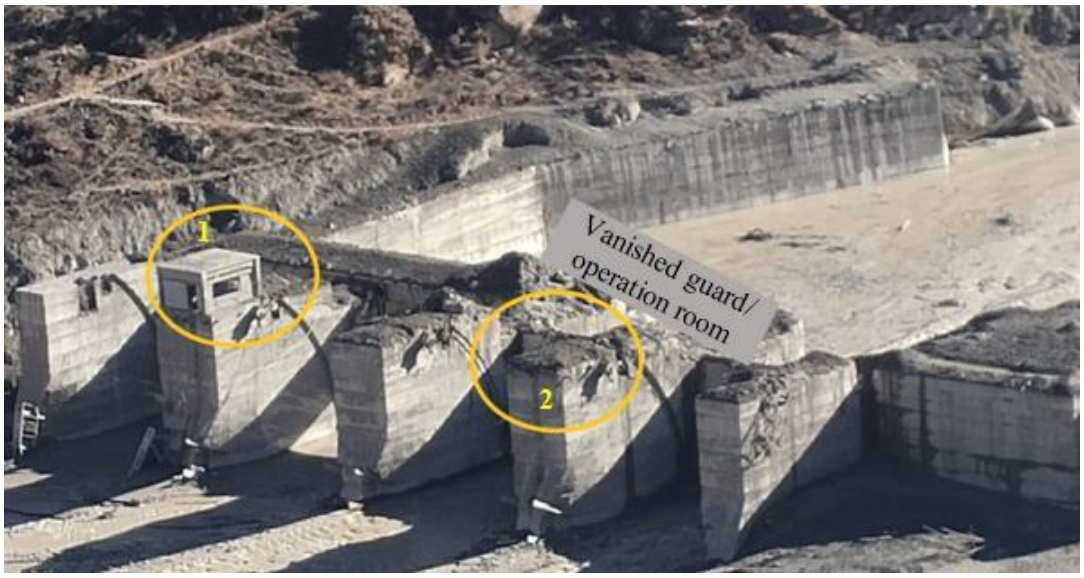

(b)

Figure 3.40 Yellow solid line circles indicating the guardrooms a) snapshot taken from a video presents the two guard rooms just before the event (Source: Sikim (native), February 7th, 2021) b) sustained and washed away guard rooms (Source: DSLR, February 11th, 2021)) @ 30°29'35.89"N 79°37'41.67"E (Dated:11/02/2021)

3.2.3.2 Bridge 1 (upstream of barrage) and 2 (downstream of barrage)

Two bridges at the entrance of Malari valley and near Tapovan have washed away. Bridge 1 was located at the upstream side of the barrage, whereas bridge-2 was downstreamof the barrage. The reconnaissance team observed during the field survey that the deck portion of both the bridges had vanished, but their piers were intact. Figure 3.41depicts the close-up of one of the collapsed bridges near the upstream of the affected site.

Figure 3.41: Close-up of collapsed bridge-1 U/s of Tapovan Barrage site(dated 11/2/21)@ 30°29'34.41"N 79°37'47.92"E

Recommendations

In June 2013, the adjoining town of Kedarnath witnessed a cascade of devastating floods and landslides that killed many people and caused large-scale destruction of bridges and roads (Allen et al., 2016; Ray et al., 2016 & Cutter et al., 2018). This previous event's flash floods and debris flow resembled the Chamoli disaster. However, the causative factors and nature are quite different (Schneider et al., 2011). To date, scores of people remain missing in the wave of water, silt, and debris that swamped the rivers and infrastructures in both events. The common factor in these events is extreme flash floods that have shown how natural events such as cloudbursts and rock-ice avalanches can be destructive. It also has opened up a new dimension for learning, taught new lessons, and attracted stakeholders' attention for future preparedness. Turning these events into knowledge is the best possible way to tackle and build resilient human-environmental interactions. To this end, the stakeholders interested in understanding the technical and causative factors of the disaster should practice conducting advanced reconnaissance studies to collect perishable and temporal data. This report demonstrated the merits of advanced drone survey data to get a preliminary understanding of the effects of the Chamoli disaster on prominent infrastructures constructed along the path of flash floods. Further, this data can also be used for research opportunities to explore more details to build resilient infrastructure and save people. The following are possible opportunities and suggestions:

- High-resolution mapping of the affected area in the future can help understand the spatial and temporal changes due to the event and monitor the area for the development of the affected area after the event.
- The DEM generated from drone imagery and Structure from Motion (SfM) technique (Lucieer et al., 2013) can be coupled with Smooth Particle Hydrodynamics (SPH) to help model and analyze the debris flow.

- Debris flows analysis from the calibrated models using actual site investigation data can help understand the flow dynamics (Evans et al., 2001) and damaging characteristics ofsuch devastating flow.
- The extent of the damage from the event can be evaluated to ensure the quality of the available avalanche and landslide susceptibility maps and identify similar locations that may be affected in future.
- Identifying the affected areas from models can help plan early warning systems and evacuation protocols, which can be made standard for other locations facing a similar danger.
- The findings highlight the fact that the large volumes of boulders, sand, and silts that construction activities excavate are usually left unmanaged along the riverbanks**.**

References

1. Allen, S. K., Rastner, P., Arora, M., Huggel, C., and Stoffel, M., 2016. Lake outburst and debris flow disaster at Kedarnath, June 2013: hydrometeorological triggering and topographic predisposition. Landslides, 13(6), 1479-1491.
2. Collins, G.S., 2015. Rock Avalanche, Encyclopedia of Planetary Landforms, Publisher: Springer New York, Pages: 1807-1811. https://doi.org/10.1007/978-1-4614-9213-9_321-1
3. Cutter, S.L., 2018. Compound, cascading, or complex disasters: what's in a name? Environment: science and policy for sustainable development, 60(6), pp.16-25.
4. Schneider, D., Huggel, C., Haeberli, W. and Kaitna, R., 2011. Unraveling driving factors for large rock–ice avalanche mobility. Earth Surface Processes and Landforms,36(14), pp.1948-1966.
5. Evans, S.G., Hungr, O., Clague, J.J., 2001. Dynamics of the 1984 rock avalanche and associated distal debris flow on Mount Cayley, British Columbia, Canada; implications for landslide hazard assessment on dissected volcanoes. Eng. Geol. 61, 29– 51. https://doi.org/10.1016/S0013-7952(00)00118-6
6. Lucieer, A., Jong, S.M.D. and Turner, D., 2014. Mapping landslide displacements using Structure from Motion (SfM) and image correlation of multi-temporal UAV photography. Progress in physical geography, 38(1), pp.97-116.
7. Martha, T.R. and Kumar, K.V., 2013. September 2012 landslide events in Okhimath, India—an assessment of landslide consequences using very high-resolution satellite data. Landslides, 10(4), pp.469-479.
8. Martha, T.R., Roy, P., Jain, N., Kumar, K.V., Reddy, P.S., Nalini, J., Sharma, S.V.S.P., Shukla, A.K., Rao, K.D., Narender, B., and Rao, P.V.N., 2021. Rock avalanche induced flash flood on 07 February 2021 in Uttarakhand, India—a photogeological reconstruction of the event. Landslides, pp.1-13. https://doi.org/10.1007/s10346-021-

01691-9

9. Naithani, A.K. and Murthy, K.K., 2006. Geological and geotechnical investigations of Tapovan-Vishnugad Hydroelectric Project, Chamoli District, Uttarakhand, India. Journal of Nepal Geological Society, 34, pp.1-16.
10. Ray, P.C., Chattoraj, S.L., Bisht, M.P.S., Kannaujiya, S., Pandey, K. and Goswami, A., 2016. Kedarnath disaster 2013: causes and consequences using remote sensing inputs. Natural Hazards, 81(1), pp.227-243.
11. Sibson, R., 1981. A Brief Description of Natural Neighbour Interpolation, Chapter 2 in Interpolating multivariate data, John Wiley & Sons, New York, pp. 21-36
12. Zwęgliński, T., 2020. The Use of Drones in Disaster Aerial Needs Reconnaissance and Damage Assessment–Three-Dimensional Modeling and Orthophoto Map Study. Sustainability, 12(15), p.6080. https://doi.org/10.3390/su12156080
13. Wartman, J., Berman, J.W., Bostrom, A., Miles, S., Olsen, M., Gurley, K., Irish, J., Lowes, L., Tanner, T., Dafni, J., and Grilliot, M., 2020. Research needs, challenges, and strategic approaches for natural hazards and disaster reconnaissance. Frontiers in Built Environment, 6, p.182. https://doi.org/10.3389/fbuil.2020.573068
14. www.thehindu.com. Accessed on 9th February 2021.